Water Resources Research

RESEARCH ARTICLE
10.1029/2025WR043105

Irrigation Monitoring With Cosmic-Ray Neutron Sensors: Unraveling Field Experiments With Neutron Transport Simulations

C. Brogi[1], F. Nieberding[1], L. Scheiffele[2,3], A. Daccache[4], M. Schrön[3], and H. R. Bogena[1]

[1]Agrosphere Institute (IBG-3), Forschungszentrum Jülich GmbH, Jülich, Germany, [2]Institute of Environmental Science and Geography, University of Potsdam, Potsdam, Germany, [3]Helmholtz Centre for Environmental Research GmbH—UFZ, Leipzig, Germany, [4]Department of Biological and Agricultural Engineering, University of California, Davis, CA, USA

Key Points:

- Cosmic-ray neutron sensor performance varies by irrigation type; hose reel raingun can show weaker, inconsistent responses
- Replacing N0 with the more modern Universal transfer solution (UTS) method improves cosmic-ray neutron sensors estimates, especially at low soil water content (SWC) levels
- Combining cosmic-ray neutron sensing with neutron transport models enhances interpretation and transferability for irrigation monitoring

Correspondence to:
C. Brogi,
c.brogi@fz-juelich.de

Citation:
Brogi, C., Nieberding, F., Scheiffele, L., Daccache, A., Schrön, M., & Bogena, H. R. (2026). Irrigation monitoring with cosmic-ray neutron sensors: Unraveling field experiments with neutron transport simulations. *Water Resources Research*, *62*, e2025WR043105. https://doi.org/10.1029/2025WR043105

Received 9 DEC 2025
Accepted 3 MAR 2026

Author Contributions:
Conceptualization: C. Brogi, F. Nieberding, H. R. Bogena
Data curation: C. Brogi, F. Nieberding, L. Scheiffele, A. Daccache
Formal analysis: C. Brogi, F. Nieberding, L. Scheiffele, M. Schrön
Methodology: C. Brogi, F. Nieberding, H. R. Bogena
Writing – original draft: C. Brogi
Writing – review & editing: C. Brogi, F. Nieberding, L. Scheiffele, A. Daccache, M. Schrön, H. R. Bogena

Abstract Irrigation is essential for stabilizing yields and sustaining food production, yet it faces increasing challenges, especially in water-scarce regions. Cosmic-ray neutron sensors (CRNS) are a promising tool in irrigation management as they can continuously monitor soil water content (SWC) over large areas. However, observational studies sometimes reported inconsistent CRNS responses across different irrigation methods and environments, limiting the broader transferability of this technique. In this study, CRNS measurements in hose reel raingun (potato), central pivot (winter wheat), and flood irrigation (alfalfa) were evaluated, and their interpretation was aided by neutron transport modeling. Overall, CRNS proved more consistent at estimating field-scale SWC than point-scale and profile sensors. Also, replacing the conventional N0 method with the Universal transfer solution approach substantially improved SWC estimates when this was below 0.10 cm^3 cm^{-3}, avoiding unrealistically low values. In flood and pivot irrigation, CRNS showed clear responses to irrigation and neutron transport simulations with the Monte Carlo code "URANOS" reproduced these dynamics well. In contrast, hose reel raingun irrigation produced weaker responses that were less consistent with URANOS, especially when irrigation occurred far from the CRNS, likely due to the co-occurrence of precipitation and the small soil volume affected by irrigation. Interestingly, a simplified analytical solution produced results comparable to URANOS, suggesting potential for rapid applications. Overall, the combination of CRNS measurements and neutron transport modeling proved key in interpreting CRNS observations across irrigation systems. Increasingly integrating observations, modeling, and recent methodological advances will likely make CRNS more transferrable, strengthening its role and adoption in irrigation management.

Plain Language Summary Efficient irrigation can be essential to ensure food production, but managing water is becoming increasingly challenging. Conventional soil water content (SWC) sensors installed directly in the soil can help managing irrigation, but they only capture small areas and can be influenced by local disturbances. In this study, we tested cosmic-ray neutron sensors (CRNS), which can continuously measure SWC over larger areas and under different irrigation systems. We also used computer simulations and simpler analytical models to help interpret the CRNS measurements. The CRNS sensors were generally more reliable than conventional sensors, especially when monitoring a potato field with strong soil roughness. The CRNS responded clearly to irrigation in flood and pivot systems, while responses were weaker under hose reel raingun, probably because only small areas were irrigated each time. Analytical models produced similar results compared to complex simulations, suggesting that rapid assessments of irrigation effects on CRNS are possible without the use of extensive computing resources. Overall, combining CRNS sensors with computer simulations provides a powerful way to better understand measurements and further support irrigation management. With continued methodological improvements, CRNS could be applied more widely and help farmers to increase crop productivity while contributing to sustainable agriculture.

1. Introduction

Agriculture is essential for human survival (European Commission: Directorate-General for Research and Innovation and Group of Chief Scientific Advisors, 2020; FAO, 2022) but faces growing challenges, including rapid population growth and increasing dependence on irrigation (Chartzoulakis & Bertaki, 2015). The global irrigated area has doubled since the 1960s with irrigated land currently producing about 40% of global food (Kamali et al., 2022; Puma & Cook, 2010; Troy et al., 2015). While irrigation helped boosting yields and

stabilizing food production, it also accounts for roughly 70% of freshwater withdrawals, half of which from non-renewable or non-local sources (Rost et al., 2008; Uhlenbrook, 2019). Additionally, inefficient irrigation can lead to water wastage, reduced yields, and soil salinization (Wichelns & Qadir, 2015), while climate change intensifies pressure on freshwater resources (Elliott et al., 2014; IPCC, 2023; Molden, 2013; Pisinaras et al., 2021). These issues are exacerbated in water-scarce regions such as South and East Asia, the Middle East, Mexico, western USA, and the Mediterranean (Bangash et al., 2013; García-Ruiz et al., 2011; Milano et al., 2013; Van Vliet et al., 2021). Addressing these challenges with sustainable irrigation practices and water-saving technologies is therefore critical (Chathuranika et al., 2022; Evans & Sadler, 2008).

One way to improve efficiency in irrigation is to accurately monitor soil water content (SWC) variations in near-real-time (Abioye et al., 2020; Adeyemi et al., 2017; Vereecken et al., 2008) for accurate irrigation scheduling management (Adeyemi et al., 2018; Dombrowski et al., 2024; Nieberding et al., 2023; Pisinaras et al., 2023; Pramanik et al., 2022). Commonly, SWC is monitored using point-measurement sensors, often deployed in arrays or sensor networks to capture within-field heterogeneity (Bogena et al., 2010; Chen et al., 2022; Majone et al., 2013). However, their high cost and restricted spatial coverage limit their effectiveness (Barker et al., 2017; Evett et al., 2009; Western et al., 2002). Alternatively, remote sensing can provide broader coverage without the logistical issues of point-scale sensors. Yet, shallow sensing depth and low temporal resolution generally constrain its usability in irrigation (Mohanty et al., 2017; Peng et al., 2021; Wagner et al., 2007; Walker et al., 2004). Methods that combine the strengths of both approaches are therefore needed. Cosmic-ray neutron sensors are a promising option, as they can bridge the gap between point-scale and remote sensing methods (M. Andreasen et al., 2017; M. J. Andreasen et al., 2017; Bogena et al., 2015; Franz et al., 2013; Hardie, 2020; Heistermann et al., 2021; Zreda et al., 2012).

CRNS measure environmental neutron intensity generated by natural cosmic radiation (Köhli, 2026; Zreda et al., 2008). As neutron intensity near the soil surface is inversely related to hydrogen abundance, CRNS provide an indirect measure of SWC (Köhli et al., 2021; Zreda et al., 2012). To enhance sensitivity to water-sensitive epithermal neutrons (0.5 eV–100 keV), CRNS are equipped with a high-density polyethylene (HDPE) moderator and sometimes an additional thermal shield that limits the influence of low-energy thermal neutrons (below 0.5 eV) (M. Andreasen et al., 2017; M. J. Andreasen et al., 2017; Desilets et al., 2010; Köhli et al., 2018; Weimar et al., 2020). A key advantage of CRNS is the large-scale sensing volume, or footprint, of 120–240 m radius and 15–85 cm depth (Köhli et al., 2015; Schrön et al., 2017). They also require little maintenance, provide continuous measurements unaffected by soil chemistry (Zreda et al., 2008) or temperature (Finkenbiner et al., 2019), and can remain in place during agricultural management (Brogi et al., 2025; Franz et al., 2016). These benefits proved valuable beyond SWC monitoring as CRNS have been used in snow monitoring (Bogena et al., 2020; Gugerli et al., 2019; Schattan et al., 2017), satellite product validation (Babaeian et al., 2018; Montzka et al., 2017), hydrological and land-surface modeling (Arnault et al., 2024; Baatz et al., 2017; Rosolem et al., 2014; Schattan et al., 2020; Shuttleworth et al., 2013), vegetation monitoring (Brogi et al., 2025; Jakobi et al., 2018, 2022; Tian et al., 2016), and to map large areas through roving surveys (Andreasen et al., 2023; Jakobi et al., 2020; McJannet et al., 2017; Schrön et al., 2021).

CRNS has strong potential for irrigation management (Franz et al., 2020; Ragab et al., 2017) and has been tested under a range of irrigation methods, including central pivot (Finkenbiner et al., 2019), variable-rate sprinkler line (Gianessi et al., 2022), linear move sprinklers (Baroni et al., 2018), mini-sprinkler (Brogi et al., 2023), and flood irrigation systems (Chen et al., 2022; Zhu et al., 2014). However, a generalized framework for precision irrigation does not currently exist and results remain inconsistent (Brogi et al., 2023). For example, while Han et al. (2016) reported potential of estimating SWC under drip irrigation, Li et al. (2019) later showed at the same field site that the sensitivity of the employed CRNS was insufficient to resolve point-scale drip irrigation under the dominant effect of the non-irrigated area. Other challenges include strong SWC heterogeneity within the CRNS footprint (Schattan et al., 2019), especially with non-radial field geometries (Schrön et al., 2023), irrigated areas smaller than the footprint (Brogi et al., 2022), or external influences from adjacent fields (Baroni et al., 2018).

Neutron transport models such as URANOS (Köhli et al., 2023) can help address these issues by simulating neutron interactions within the soil–vegetation–atmosphere continuum, thereby aiding the interpretation of CRNS data in irrigated environments. Although URANOS has been applied in over 30 studies (URANOS, 2025), only a

Table 1
Manufacturers, Models, and Characteristics of the Cosmic-Ray Neutron Sensors Used in This Study

Manufacturer	Model	Method	Moderator	Cts/h
StyX Neutronica	System S1	B_4C	25 mm	1,000
StyX Neutronica	System SP	B_4C	25 mm	2,300
Finapp	Finapp 3	Scintillator	15 mm	900
Hydroinnova	CRS 1000	^{3}He	25 mm	775[a]

[a]Estimated count rate, as a value is not currently provided in manufacturer's website.

few have focused on irrigation to either explain (Li et al., 2019) or improve (Brogi et al., 2023) field-based CRNS estimates, or to assess irrigation feasibility and heterogeneity in synthetic experiments (Brogi et al., 2022; Francke et al., 2025; Schrön et al., 2023). Further research is thus needed to better understand CRNS responses under different irrigation settings. Within this context, the goals of this study were to:

1. Evaluate the performance of different CRNS setups across three irrigation systems and crop types in comparison to a limited number of point-scale sensors;
2. Assess the ability of URANOS neutron transport simulations (Köhli et al., 2023) and of the analytical signal contribution concept (Schrön et al., 2023) to explain CRNS observations and capture the effects of SWC sub-footprint heterogeneity;
3. Explore whether combining measurements and simulations can provide key insights and improve the transferability of CRNS-based irrigation monitoring.

In this study, three different irrigated fields where irrigation is managed by the field owner were monitored: a potato field in western Germany with hose reel raingun (three CRNS, six profile sensors), a winter wheat field in eastern Germany with central pivot irrigation (one CRNS, one profile sensor), and an alfalfa field in California, US, with flood irrigation (one CRNS, two point-scale sensors). The five CRNS that were used are from three manufacturers and are considered comparable in SWC estimation. Neutron transport and detection were simulated with URANOS for all sites and compared with field measurements. In the potato field, an analytical signal contribution approach was also applied and compared with URANOS results.

2. Materials and Methods

2.1. Soil Water Content Monitoring Instrumentation

2.1.1. Cosmic-Ray Neutron Sensors

Cosmic-ray neutron sensing (CRNS) for soil water content (SWC) monitoring is a passive technology based on the detection of natural and omnipresent neutron radiation (Zreda et al., 2012). Neutrons produced by cosmic-ray particle showers in the atmosphere interact with the soil in depths of up to 1 m. Here, hydrogen atoms slow down these neutrons and can prevent them from escaping the soil. Epithermal neutrons (from 1 eV to 100 keV) that escape the soil will scatter horizontally across hundreds of meters (Köhli et al., 2015) and represent a proxy for average SWC in the upper soil horizons and within hectares around the sensor. This detection method is non-invasive, requires low power and maintenance, and is continuous in time.

In this study, CRNS from three manufacturers were used: a) StyX Neutronica GmbH (Mannheim, Germany), b) Hydroinnova LLC (Albuquerque, NM, USA), and c) Finapp srl (Montegrotto Terme, Italy). Instrument details such as the thickness of the HDPE moderator are specified in Table 1. StyX Neutronica instruments (S1 and SP) were equipped with proportional counting tubes coated with boron carbide (B_4C) enriched to 96% in ^{10}B and serving as the neutron converter that is filled with an argon–CO_2 mixture as the counting gas (Weimar et al., 2020). These had an additional gadolinium oxide-based (Gd_2O_3) thermal shield (Ney et al., 2021). The Hydroinnova instrument (CRS 1000), instead, had Helium-3 (^{3}H) as detector gas in its proportional counter tubes, which makes the system more lightweight compared to ^{10}B detectors. The Finapp instrument (Finapp3) is more compact than the others due to the use of a layered structure of stable lithium 6-fluoride (^{6}LiF) and a zinc sulphide phosphor (ZnS:Ag) scintillator (Gianessi et al., 2022). The typical hourly count rates (Cts hr^{-1}) provided on the manufacturers' websites are reported in Table 1. The count rate of the CRS 1000 was not provided by the manufacturer's website. Thus, an estimation was obtained from an available data set in which a CRS 1000, two SP1, and two Finapp3 were compared (data not shown). It is important to note that, as there is no common standard for typical neutron count rates, the rates from different manufacturers in Table 1 should not be directly compared. Also, these rates become relevant when sensors are installed in close proximity and soil moisture is derived using a single calibration parameter (Heistermann et al., 2021), which is not the case in this study. Each

Table 2
Manufacturers, Models, and Characteristics of the Point-Scale and Profile Sensors

Manufacturer	Model	Type	Fixed sensing depths (cm)
Sentek Pty	Drill&Drop	FDR	5-15-25-35-45-55
Campbell Scientific	SoilVUE10	TDR	5-10-20-30-40-50
Delta-T Devices	PR2/6 SDI	FDR	10-20-30-40-60-100
Meter Group	ECH$_2$O EC-5	FDR	Non-Fixed Depth

CRNS was equipped with a logger that records neutron count rates every 15 or 20 min. Measurements were then transmitted hourly via NB-IoT or 4G networks.

2.1.2. Point-Scale Soil Water Content Sensors

In this study, profile sensors from three manufacturers were used: a) Campbell Scientific Inc. (Logan UT, USA), b) Sentek Pty Ltd. (Stepney, Australia), and c) Delta-T Devices LLC (Cambridge, UK). These consist of elongated probes with sensing elements at fixed depths. Additionally, conventional point-scales sensors from Meter Group Inc. (Pullman, WA, USA) were employed. In this case, multiple point-scale sensors can be installed at variable depths at the same location. Instruments used either Frequency Domain Reflectometry (FDR) or Time Domain Reflectometry (TDR) techniques (see Table 2). Further details on sensor specifications and accuracy are provided in Nieberding et al. (2023).

2.2. Investigated Fields

The three investigated fields were monitored in 2023 and are a) a potato field irrigated with continuous hose reel raingun in Leerodt, Germany (Figure 1a), b) a winter wheat field irrigated with central pivot system in Oehna, Germany (Figure 1b), and c) an alfalfa field in Davis, USA, where flood irrigation is performed (Figure 1c).

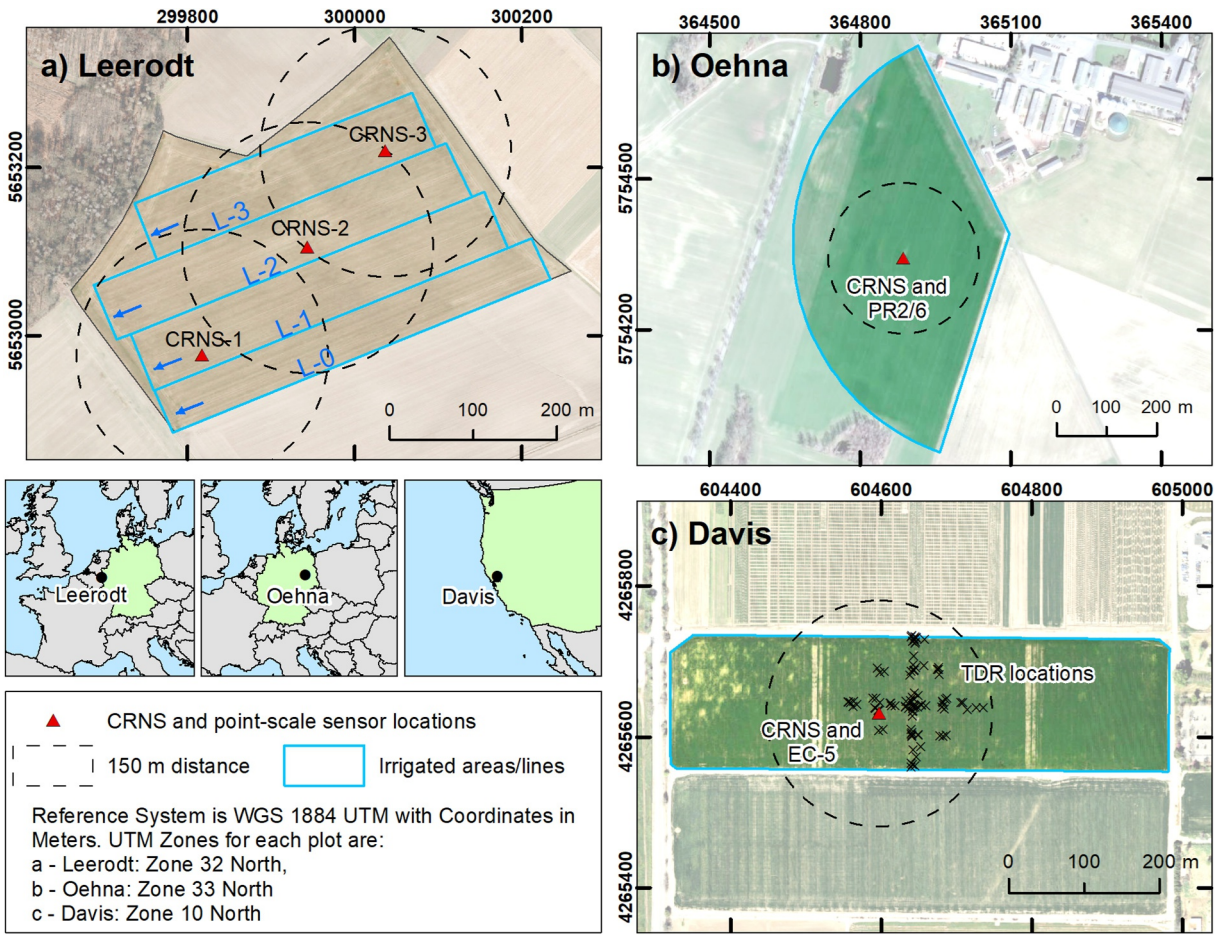

Figure 1. Overview of the three study sites in panel (a) Leerodt, (b) Oehna, and (c) Davis. The position of the Cosmic-ray neutron sensors (CRNS) and of the co-located point-scale sensors are indicated together with a 150 m radius from the CRNS and with the geometry of the irrigated areas. In the case of Leerodt, the four irrigation lines are shown separately and named L0 to L3 with blue arrows indicating irrigation direction.

2.2.1. Leerodt Potato Field (Hose Reel Raingun)

The Leerodt field (50.9945°N, 6.1488°E, 80 m a.s.l.) measures 14 ha (Figure 1a) and was planted with potato on 25th May and harvested on 20th October 2023. The local climate is temperate oceanic (Cfb on Koppen climate classification), with an annual mean temperature and precipitation of approximately 10.9°C and 789 mm, respectively. The soils are Luvic-Stagnosols with varying gravel content above early Pleistocene river deposits. Detailed soil information for the area is available in the German Bodenkarte 1:5000 (BK5), which was obtained as WMS service from the Geological Survey of North-Rhine Westphalia (NRW, 2025) and digitized using ArcGIS version 10.7.1 (ESRI Inc., Redlands, CA, USA). From July 2023, the field was irrigated using a hose reel raingun system operating along four lines, each 72 m wide (referred to as L-0, L-1, L-2, and L-3 in Figure 1a). Each line was irrigated for several hours on separate, non-consecutive days. The amount of irrigated water was recorded and converted to millimeters using the Raindancer irrigation control device (IT-Direkt Business Technologies GmbH, Berlin, Germany), which was mounted directly on the raingun system.

In March 2023, electromagnetic induction (EMI) measurements of apparent electrical conductivity (ECa) were collected to assess soil heterogeneity (Corwin & Lesch, 2003). For this, a 3-coil CMD-MiniExplorer and a 6-coil CMD-MiniExplorer Special-Edition (GF Instruments s.r.o., Brno, Czech Republic) were used, resulting in depths of investigation (DOI) ranging from 0 to 270 cm (McNeill, 1980). A more in-depth description of the measurement methodology and instrumentation can be found in Appendix B as well as in von Hebel et al. (2018), Brogi et al. (2019), Kaufmann et al. (2020), and Schmäck et al. (2022).

On 24th May 2023, immediately after sowing, three measurement locations named CRNS-1, CRNS-2, and CRNS-3 were selected (Figure 1a). At each of these locations, a Drill&Drop and a SoilVUE10 sensors were installed above the ridges where potatoes were planted. For the Drill&Drop sensors, the "combined Sentek D&D calibration" from the instrument manual was employed. For the SoilVUE10 sensors, a standard factory calibration was used and the sensor output was subsequently related to SWC using the Topp equation (Topp et al., 1980). Then, two StyX Neutronica S1 were installed at locations CRNS-1 and CRNS-3 (within L-1 and L-3) and a StyX Neutronica SP was installed at location CRNS-2 (within L-2). The sensors were positioned away from the center of irrigation lines to not interfere with field management. Thus, location CRNS-1 was closer to L-0 than to L-2, CRNS-2 was closer to L-1 than to L-3, and CRNS-3 was closer to L-2 than to the field border. SWC measurements were conducted continuously until harvest, and each location was periodically visited to observe the conditions of the instruments. Location CRNS-2 was additionally equipped with an ATMOS41 (METER Group, Inc., Pullman, WA, USA) all-in-one weather station to record air temperature, relative humidity, and atmospheric pressure at 2-m height.

2.2.2. Oehna Winter Wheat Field (Pivot System)

The Oehna field (51.9234°N, 13.0351°E, 85 m a.s.l) measures 30 ha and is irrigated with central pivot sprinklers. The climate is humid continental (Dfb), with a mean annual temperature of 9.6°C and 540 mm of annual precipitation (DWD weather station Langenlipsdorf, averaged over 1991–2020). The soil is classified as Brunic Arenosols derived from glacial sediments, with a loamy sand texture (derived from the state's soil map BUEK300 (LBGR, 2025)). From 27th September 2022, the field was cropped with winter wheat, which was harvested on 22nd August 2023. Winter wheat was irrigated five times between 18th May and 17th June 2023, with irrigation amounts ranging between 14 and 26 mm per event (personal communication with the farmer). In December 2021, a CRS1000 was installed in the center of the field and nearby a PR2/6 profile probe (Figure 1b). The PR2/6 readings at each sensing depth were calibrated using the air-water normalization procedure of Kootanoor Sheshadrivasan et al. (2025). During the winter wheat season, the PR2/6 measured SWC only at 10, 20, 30, and 40 cm depth as the sensor rings at 60 and 100 cm had previously failed due to corrosion. Both instruments were installed in a small, uncultivated area of a few square meters. Air temperature and relative humidity were recorded with sensors co-located with the CRNS and precipitation data was obtained from the DWD weather station Langenlipsdorf, located approximately 4 km east of the field site.

2.2.3. Davis Alfalfa Field (Flood Irrigation)

The study site in Davis (38.5330°N, 121.7993°W, 20 m a.s.l) is a 12-ha field of flood irrigated alfalfa crop. The climate is typical Mediterranean (Csa), characterized by long, hot summers and mild wet winters. Average daily temperatures vary from 33.4°C in July and 13.1°C in January while the average annual precipitation is around

487 mm, mostly falling between mid-November and mid-March. The soil is predominantly Silty Clay with a stretch of the field classified as Silty Clay Loam under the USDA soil texture classification. Generally, four to five alfalfa cuts are performed annually. The field is divided in three sectors. After each cut, irrigation is performed via gated pipes installed along the southern border of the field. On 24th May 2023, a Finapp3 CRNS was installed in the center of the field. Nearby the CRNS, two ECH_2O EC-5 sensors were placed at 5 and 10 cm depths (Figure 1c). The typical factory calibration function was used for these ECH_2O EC-5 sensors. Air temperature and humidity were recorded with a Hygrovue10 sensor (Campbell Scientific Inc., Logan, UT, USA) while precipitation was recorded with a TE525 WS-L rain gauge tipping bucket (Campbell Scientific Inc., Logan, UT, USA). On four days during the irrigation season, TDR measurements of SWC at the soil surface were performed within the central portion of the field (black crosses in Figure 1c). For each measurement day, the average value of the TDR readings was obtained.

2.3. CRNS Data Management and SWC Estimations

Measured neutron counts were processed in accordance to the method applied for most Europe-based sensors by following Bogena et al. (2022). Raw measurements from each CRNS were aggregated to hourly time steps and converted to raw neutron counts per hour (N_r). After removing outliers with a max-min filter, N_r higher (or lower) than a 24-hr moving average plus (or minus) twice the standard deviation of this 24-hr moving average were also removed. To correct N_r for environmental variables, the atmospheric pressure C_p (Desilets & Zreda, 2003), air humidity C_h (Rosolem et al., 2013), an incoming neutron C_i (McJannet & Desilets, 2023) correction factors were calculated at each time step using:

$$C_p = e^{\beta(P-P_0)} \tag{1}$$

$$C_h = 1 + \mathrm{ah} \tag{2}$$

$$C_i = (\tau I / I_{\mathrm{ref}} + 1 - \tau) \tag{3}$$

where β is the barometric coefficient, assumed to be equal to 0.0076 hPa^{-1}, P and P_0 are the actual and reference atmospheric pressure in hPa, a is set to 0.0054 $\mathrm{m}^3\ \mathrm{g}^{-1}$, h is the absolute humidity in g m^{-3}, I is the incoming count rate measured at the Jungfraujoch neutron monitor in Switzerland, I_{ref} is the incoming count rate at an arbitrary time, and τ is a location-specific scaling factor accounting for the different cosmic-ray shielding at different places on Earth (calculated using an online tool accessible at https://crnslab.org/util/tau.php). The Jungfraujoch neutron monitor was used because it provides high-quality, continuous data, is representative for Europe (McJannet & Desilets, 2023), and has a geomagnetic cut-off rigidity similar to that of Davis (4.13 GV). Moreover, in the Davis case, data from three additional neutron monitors were used: Calgary (CALG), Mexico City (MXCO) and Newark (NEWK). These factors were then used to obtain corrected neutron counts N_{phi} from N_r:

$$N_{\mathrm{phi}} = N_r * C_p * C_h * C_i \tag{4}$$

Vegetation correction was not applied because sufficiently detailed biomass information was unavailable. In addition, some CRNS were equipped with a thermal shield to reduce the influence of nearby vegetation on the measured count rate. Measured and corrected neutron counts were converted to SWC estimates by using two different approaches. The first approach by Desilets et al. (2010) has been used frequently in the past, but is known to have shortcomings for very dry conditions. In this approach, a 24-hr running average was applied to N_{phi} to reduce noise and measurement uncertainty (Zreda et al., 2008). Then, SWC (θ) was estimated using:

$$\mathrm{N_0\ approach}: \theta(N) = \varrho_s\left(a_0(N_{\mathrm{phi}}/N_0 - a_1)^{-1} - a_2\right) - \theta_{\mathrm{off}} \tag{5}$$

where ϱ_s is the soil bulk density, parameters a_0, a_1, and a_2 follow the values from Desilets et al. (2010), θ_{off} is the volumetric soil moisture equivalent of lattice water and soil organic matter (Franz et al., 2012), and N_0 is the count rate over dry soil.

The second approach utilizes the Universal Transfer Solution (UTS) by Köhli et al. (2021), which is a revised function valid also for dry conditions, accounting explicitly for the dependence of neutron transport on absolute

humidity. Since it already includes a more complex correction for air humidity, the previous correction approach (Equation 2) is ignored (i.e., $N_{\mathrm{pi}} = N_r * C_p * C_i$):

$$\text{UTS approach}: \theta(N) = f^{-1}\left(N_{\mathrm{pi}}/N_D, h, \varrho_s\right) - \theta_{\mathrm{off}} \tag{6}$$

where h is the absolute air humidity. For Equation 6, instead of smoothing N_{pi}, a 24-hr running average was applied after conversion to SWC. The function $f(\theta, h) \rightarrow N_{\mathrm{pi}}/N_D$ is the UTS function defined in Köhli et al. (2021) using the parameter set "mcnp drf" (for a more detailed description on applying the UTS approach see Rasche et al. (2024)). N_0 and N_D are neutron scaling parameters for the two respective approaches, roughly representing the count rate over dry soil, which mainly depends on the detector type.

2.4. Calibration of CRNS Measurements

An appropriate calibration of the neutron scaling parameters N_0 and N_D for each CRNS is required to obtain accurate SWC estimates from measured neutron counts. For each CRNS instrument, 18 locations were selected at distances that ranged from 2 to 120 m to account for the horizontal sensitivity of the CRNS and to better capture SWC heterogeneity (Schrön et al., 2017). Calibration took place on 1st June 2023 in Leerodt, on 29th March 2022 and 4th May 2025 in Oehna, and on 6th September 2023 in Davis. In Leerodt, soil cores of 30 cm depth and 5 cm diameter were collected at each location. The soil cores were divided into 5 cm long segments and oven-dried at 105°C for 24 hr to obtain gravimetric SWC (θ) and ϱ_s. In Oehna, the same approach was used but, for the second campaign, the soil sampling was partially replaced by determining depth specific soil moisture with a handheld FDR ThetaProbe ML2x (Delta-T Devices LLC, Cambridge, UK). A similar approach was applied in Davis by using a TDR Fieldscout 350 (Spectrum Technologies Inc., Aurora IL, USA) at depths of 8 and 20 cm. In Leerodt and Davis, θ_{off} was obtained from clay content information contained in soil maps (Dong & Ochsner, 2018). In Oehna instead, the loss-on-ignition method was applied to depth-specific composite samples (Heidbüchel et al., 2016; Scheiffele et al., 2020). In all fields, a 1% SOC content was assumed as this is generally consistent with these areas and with agricultural management (Brogi et al., 2025).

The sensitivity of the CRNS decreases with increasing depth and distance from the sensor (Köhli et al., 2015; Schrön et al., 2017). Therefore, a vertical and horizontal weighting and averaging were applied to θ, ϱ_s, and θ_{off} for each of the 18 locations. A detailed description of the calibration and distribution of soil samples can be found in Schrön et al. (2017). During the calibration process, Equation 5 and Equation 6 are solved for N_0 and N_D respectively, using the θ, ϱ_s, and θ_{off} obtained from the soil samples. Simultaneously, the average N_{phi} measured on the sampling day is used in the N0 approach while average N_{pi} and average absolute humidity are used in the UTS approach. For Oehna, the averages of both calibration parameters from the two available campaigns were used.

2.5. Neutron Transport Simulations

Neutron transport simulations were performed using the Monte Carlo-based URANOS model (Köhli et al., 2023), a free software package specifically developed for CRNS studies. It offers a high computational efficiency, and the simulation results can be tailored to a given CRNS design by using CRNS-specific response functions in post-processing. In each of the three study areas, simulations featured a square domain of 1,200 × 1,200 m. The atmospheric layer extended from the ground to 1,000 m height while the soil layer reached up to 1.6 m depth. The detectors (either detector voxels, or a cylindrical detector volume) were placed between 1 and 2 m above the ground while the source layer extended between 50 and 80 m height. Each study area was divided in land use classes by digitizing satellite images (ESRI, 2025). These classes included trees (10 m height, 3 kg m^{-3} biomass), agriculture (1 m height, 5 kg m^{-3} biomass), grass (0.1 m height, 5 kg m^{-3} biomass), low buildings (5 m height), high buildings (10 m height), and bare soil. The land use polygons were then converted to raster format at appropriate resolution using ArcGIS version 10.7.1. In each field, the URANOS results were compared with measured neutron counts to evaluate the model ability of reconstructing measured patterns and to investigate the sensitivity of CRNS to irrigation. This was done by estimating the percentage of variation between simulated scenarios and by applying these variations to measured counts, starting with 100% detection for dry, initial conditions. The relative errors of the simulations were calculated using initial and final SWC conditions as done in (Brogi et al., 2022).

2.5.1. Leerodt Field

URANOS (version 1.23) simulations of the Leerodt field had a horizontal resolution of 10 m, which balanced sufficient neutron detection with computational efficiency. To represent all the three CRNS in a single simulation run, a $10 \times 10 \times 1$ m detector voxel was positioned at each CRNS locations (1–2 m above the ground). Given the separate irrigation of parts of the field, a relatively complex distribution of SWC is expected in Leerodt compared to the other study areas. Thus, a simple yet sufficiently accurate representation of SWC dynamics between dry periods, irrigation, and precipitation was achieved by combining soil unit geometry and texture from the local BK5 with the ECa maps recorded with EMI. Additional details on the construction of the domain are provided in Appendix B. This procedure enabled reconstruction of SWC across the domain for six scenarios:

1. Dry conditions prior to irrigation or precipitation;
2. 25 mm irrigation of line L-0;
3. 25 mm irrigation of line L-1 and partial dry-out of line L-0;
4. 25 mm irrigation of line L-2 and partial dry out of lines L-0 and L-1;
5. 25 mm irrigation of line L-3 and partial dry out of lines L-0, L-1, and L-2;
6. Wet conditions caused by 30 mm precipitation.

For each scenario, 500 million neutrons were simulated and, for neutrons passing the detector, the energy at detection was used to reconstruct the number of detected neutrons. For this, a response function of a Boron-lined proportional counter tube with a 25 mm HDPE moderator and Gadolinium shield was used (Weimar et al., 2020). Moreover, the coordinates of the first soil contact of detected neutrons were used to reconstruct the contribution to detection of each irrigation line of the Leerodt field and of the non-irrigated area.

In addition to URANOS simulations, estimated contributions of irrigation were calculated based on the signal contribution concept by Schrön et al. (2023). The advantage of this analytical approach is that results can be calculated directly without computationally expensive Monte Carlo simulations. Similarly to the case of the URANOS simulations, the approach was used to estimate the CRNS response to irrigation in different areas of the Leerodt field site. For this, the same domain as that of the URANOS simulations was used, although without land use information and with a higher horizontal resolution of 1 m. The approach of Schrön et al. (2023) currently assumes a homogeneous soil profile. To mimic the stratified soil moisture changes in such a homogeneous profile, three separate instances were calculated using a) SWC from 0 to 30 cm depth (equal to URANOS first soil layer), b) SWC integrated over 50 cm depth, and c) SWC integrated over 80 cm depth. The results were then compared with those of the URANOS simulations.

2.5.2. Oehna Field

For the Oehna field, URANOS (version 1.27) simulated 300 million neutrons, had a horizontal resolution of 1 m, and used a cylindrical detector of 9 m radius positioned at the center of the domain. Three scenarios were constructed using SWC values for dry, irrigation, and precipitation periods, obtained from the point-scale measurements. The response function of a Helium-3 proportional counter tube with 25 mm HDPE moderator (courtesy of Daniel Rasche) was used to derive detected neutrons.

2.5.3. Davis Field

For the Davis field, URANOS (version 1.27) simulated 300 million neutrons, had a horizontal resolution of 1 m, and used a cylindrical detector of 9 m radius at the center of the domain. Three scenarios were constructed with SWC values for dry periods, irrigation, and irrigation of a nearby field, obtained from the point-scale measurements. Additionally, to mimic flood irrigation, a 2 cm layer of water was added on top of the irrigated field. This water layer was not included in the nearby field as it is irrigated with a lateral move sprinklers system. Detected neutrons were determined by using the response function of a Finapp3 sensor (courtesy of Marcello Lunardon).

3. Results and Discussion

3.1. SWC Measurements and Irrigation Monitoring With CRNS

Regarding the CRNS data management, the outliers filtering applied to measured neutron counts resulted in the removal of 3.1%, 3.7%, and 3.6% of values in Leerodt locations CRNS-01, CRNS-02, and CRNS-03,

respectively. In Oehna, this was 2.9%, and in Davis it was 1.6%. Importantly, none of these outliers occurred during irrigation events.

3.1.1. Leerodt Field

SWC measurements in the Leerodt field during the 2023 potato growing season are shown in Figure 2. Irrigation was first applied to line L-0 on July 6th, followed by L-1 on July 12th, L-2 on July 13th, and L-3 on July 15th. A second round of irrigation occurred on July 24th on L-0 and July 26th on L-1. Subsequent frequent rainfall maintained relatively high SWC, and no further irrigation was required until a single event in L-2 on August 24th. Such a rainfall pattern was unusual for the region, where potatoes are typically irrigated in both July and August due to limited precipitation.

Point-scale profile measurements of SWC by Drill&Drop and SoilVUE10 sensors (Figures 2d–2i) show contrasting performance across the three monitored locations. At location CRNS-1, Drill&Drop measurements closely reflected precipitation and irrigation events, with pronounced dynamics at 5 and 15 cm and a gradual decline at deeper depths until late July. In contrast, the SoilVUE10 frequently recorded implausibly low SWC at 5 and 10 cm, likely due to poor soil contact caused by loose ridges and erosion of the potato dams (see Appendix A). At CRNS-2, the Drill&Drop showed limited response to precipitation and irrigation at shallow depths, while SoilVUE10 measurements up to 20 cm remained near 0 cm^3 cm^{-3}, indicating generally poor soil contact for both instruments, probably due to ridge erosion and soil shrinkage. At CRNS-3, the Drill&Drop measurements appeared more reliable, with consistent dynamics at shallow depths and stable SWC below 25 cm. The SoilVUE10 measurements below 20 cm remained stable, but shallow measurements again showed unrealistically low values a few weeks after installation, likely due to installation issues or soil incompatibility.

CRNS measurements at the three sites using the N0 and UTS approaches are shown in Figures 2b and 2c. Estimated SWC generally declined during early June, then increased following precipitation and irrigation events in late June and July. From late July onward, frequent rainfall caused sharp increases in SWC, followed by gradual dry-down and clear responses to intense rain events in late August and September. This was particularly the case in CRNS-2, which show higher SWC estimates because it is located in a slight depression at the center of the field where more water can accumulate. While estimates from the UTS approach are generally lower during wet periods, the differences with the N0 approach are minimal, especially during the irrigation period. However, it should be noted that SWC ranged between 0.15 and 0.20 cm^3 cm^{-3} during the irrigation period, and the N0 and UTS approaches are expected to provide similar estimates within this SWC range (Köhli et al., 2021). Each CRNS was most responsive to irrigation within its own line, reflecting stronger sensitivity to nearby soil conditions, although rainfall likely dampened the influence of irrigation applied to adjacent lines. Among the three instruments, the two-tube CRNS at location CRNS-2 showed the strongest responses to irrigation, likely due to both its higher count rate and central position in the field (Figure 1a).

Overall, point-scale measurements with soil profile sensors were strongly affected by loss of soil contact, particularly at shallow depths (see Appendix A). At depths of 20 cm and below, SWC were generally stable, although inconsistent readings from nearby sensors indicate that these measurements may still be somewhat unreliable. Although frequent reinstallation could have improved soil contact, this was not feasible in the present study. In contrast, despite their inherently lower spatial and depth resolution, the three CRNS provided continuous and more consistent estimates of SWC, suggesting that they could be better suited for monitoring soil water dynamics during irrigated periods for the investigated field.

3.1.2. Oehna Field

SWC measurements in the Oehna field during the 2023 winter wheat growing season are shown in Figure 3. Five irrigation events occurred between May 18th and June 17th. Then, a large precipitation event on June 22nd to 23rd substantially increased SWC, and no further irrigation was required until harvest. The PR2/6 profile sensor captured SWC dynamics that were consistent with the irrigation period, showing variations at 10 and 20 cm depths and relatively stable values at 30 and 40 cm depths (lower panel in Figure 3). The intense June 22nd to 23rd rainfall affected all measurement depths. Following this event, SWC dropped sharply at approximately 30 cm, with implausible values near 0 cm^3 cm^{-3}. Sensor readings appeared to have deteriorated after the intense rainfall event, likely due to moisture entering the access tube. Although the values stabilized later in the season, complete sensor malfunction a few months later necessitated its replacement (data not shown).

10.1029/2025WR043105

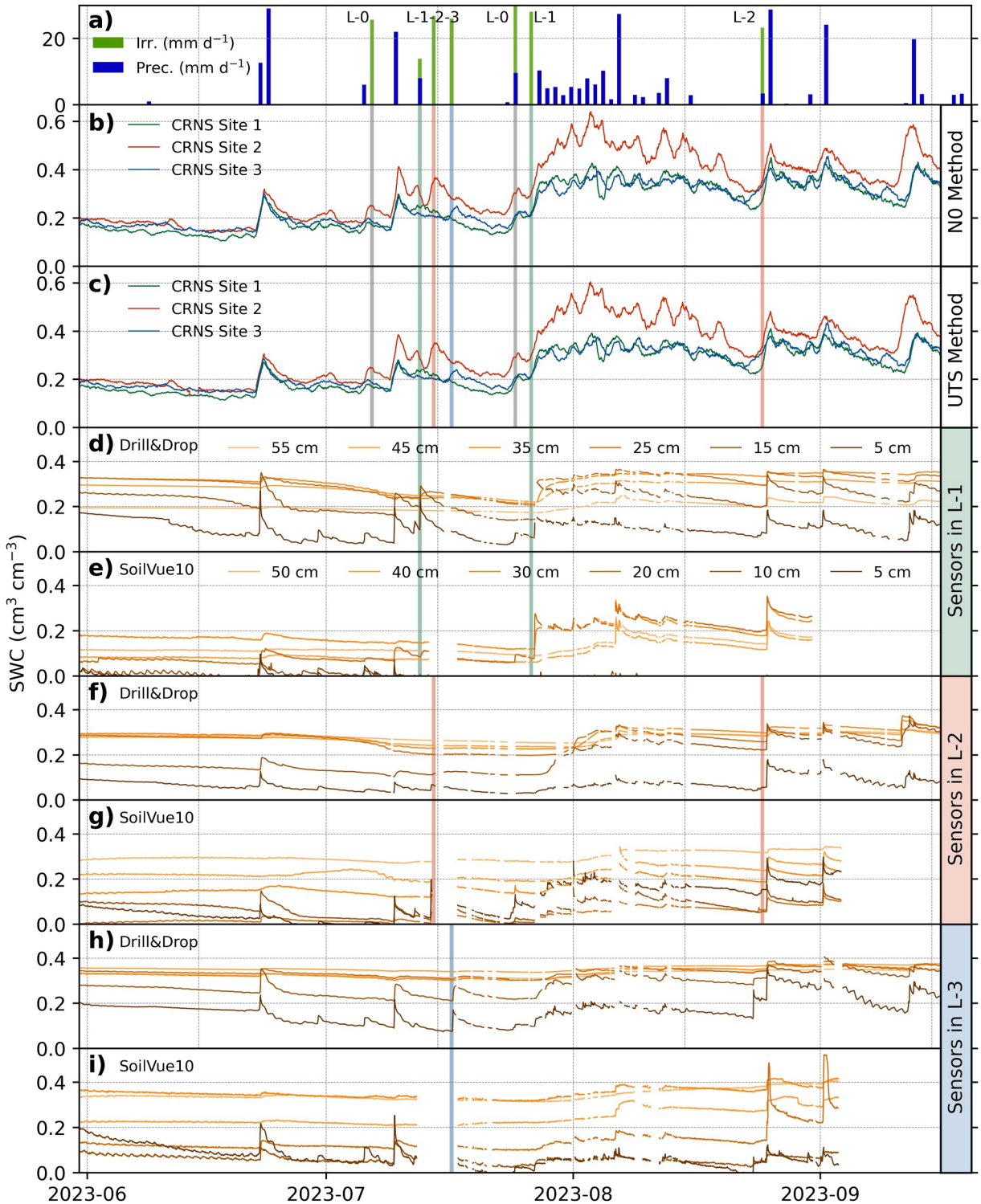

Figure 2. Precipitation, irrigation, and soil water content (SWC) measurements in the Leerodt field. Plot (a) shows precipitation and irrigation. Plot (b) shows SWC estimated by the three Cosmic-ray neutron sensors (CRNS) using the N0 approach while plot (c) shows SWC estimated with the Universal Transfer Solution approach. Throughout plots (b, c), colored areas show irrigation events with the color matching the CRNS location. SWC measured by the Drill&Drop and SoilVUE10 at multiple depths is shown in plots (d, e) for location CRNS-1, (f, g) for CRNS-2, and (h, i) for CRNS-3. Throughout plots (d–i), colored areas show the irrigation events that occurred at the sensor locations.

10.1029/2025WR043105

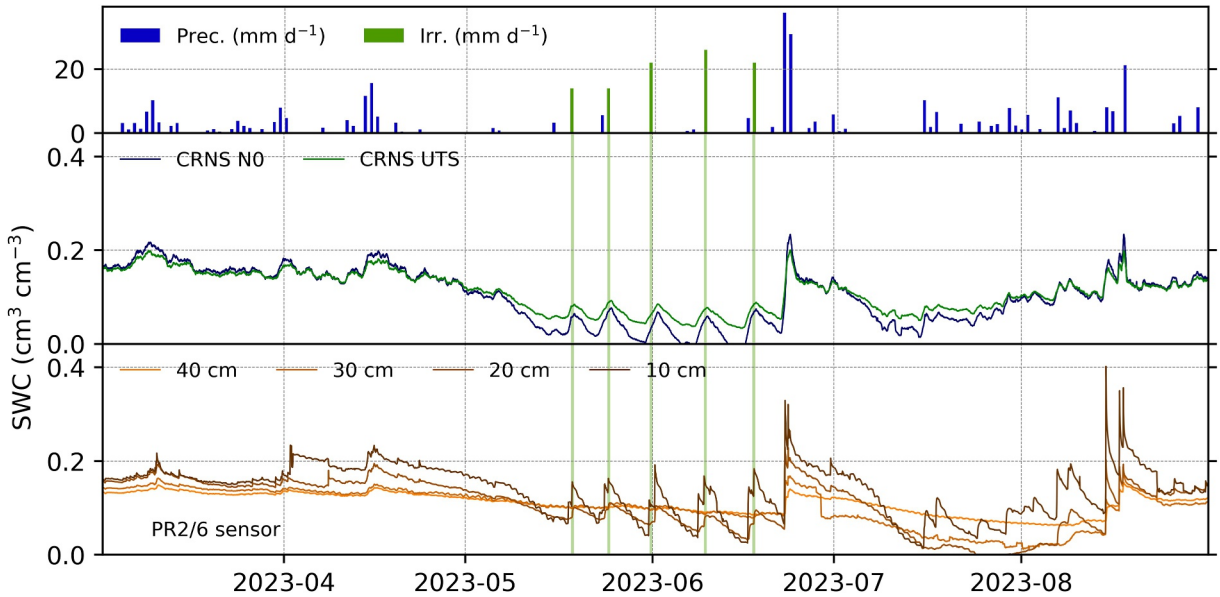

Figure 3. Precipitation, irrigation, and soil water content (SWC) measurements in the Oehna field. Top plot shows precipitation and irrigation. Central plot shows SWC estimated by the Cosmic-ray neutron sensors using the N0 and Universal transfer solution approach. SWC measured by the PR2/6 profile sensors is shown in lower plot.

CRNS estimates of SWC are shown in Figure 3 (central panel). SWC was relatively high before and after the irrigation period, and the N0 and UTS approaches produced similar estimates. However, during the drier irrigated period, the two approaches diverged: N0-based SWC exhibited stronger dynamics but also unrealistic low values (even below 0 cm^3 cm^{-3}), whereas UTS-based SWC showed smaller, more plausible variations. The UTS estimates were more consistent with PR2/6 sensor measurements and with the fact that CRNS integrates SWC over several hectares and decimeters of depth. These observations confirm the findings of Rasche et al. (2024) who showed that the UTS approach provides more reliable estimates during dry periods, while the N0 approach likely overestimates SWC dynamics. Overall, CRNS and point-scale measurements were generally consistent and could both be used to monitor soil water and inform irrigation in this field. Nonetheless, the quality of point-scale measurements degraded after the June 22nd—23rd rainfall, which could have posed greater challenges had it occurred earlier or during the irrigation season.

3.1.3. Davis Field

SWC measurements in the Davis field during summer 2023 are shown in Figure 4. Five flood irrigation events occurred between June 13th and October 21st. ECH_2O EC-5 sensors captured SWC changes primarily during these irrigation events, while precipitation events had little effect (lower plot in Figure 4). In contrast, CRNS measurements showed more dynamic SWC estimates (central plot in Figure 4). Both techniques were generally consistent with distributed and averaged TDR measurements (black crosses in Figure 1c) at four dates (red points and error bars in Figure 4), that represent the overall SWC conditions of the field at the soil surface. Nonetheless, the CRNS showed a slightly better match, whereas point-scale sensors underestimated SWC at times. The generally lower dynamics observed in the ECH_2O EC-5 sensors are likely due to their placement at a single location and under vegetation cover, which can dampen responses to rainfall and other environmental effects. These results suggest that the CRNS provided more representative field-scale SWC estimates. Nonetheless, both instruments provided sufficiently reliable measurements for this field and irrigation method.

Following the irrigation event on September 13th, the CRNS recorded three consecutive SWC increases that were not consistent with point-scale and TDR measurements. During this period, several irrigation events were reported in a nearby field approximately 100 m north of the CRNS, occurring between 15th and 30th September. The potential influence of this adjacent irrigation is explored in the following section.

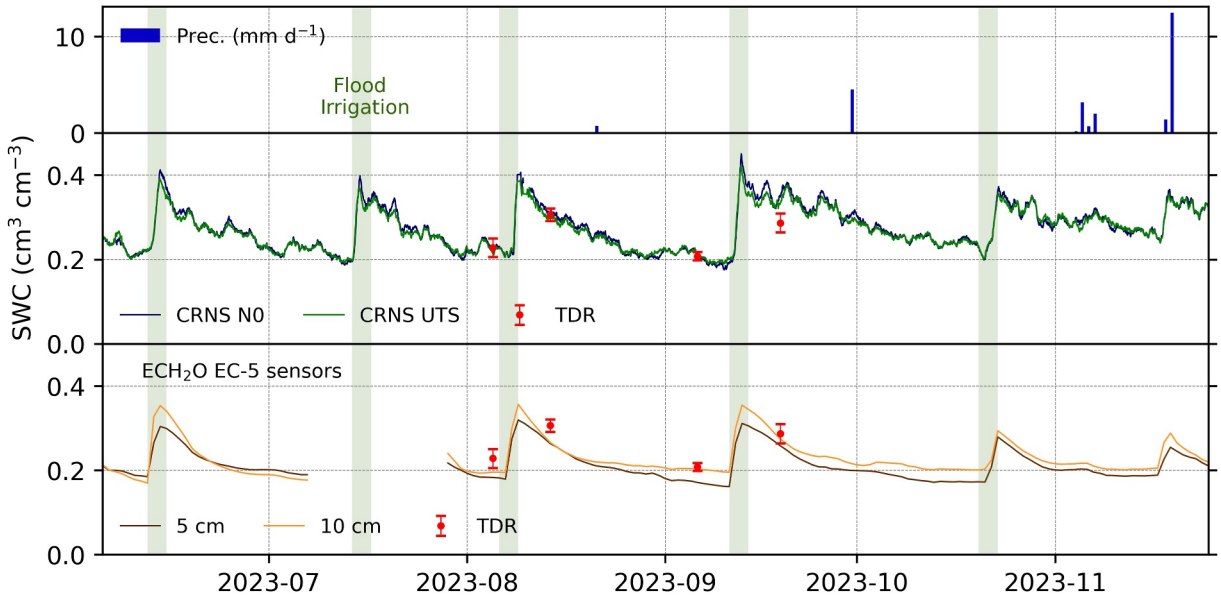

Figure 4. Precipitation, irrigation, and soil water content (SWC) measurements in the Davis field. Top plot shows precipitation and irrigation. Central plot shows SWC estimated by the Cosmic-ray neutron sensors using the N0 and Universal transfer solution approaches. SWC measured by the ECH2O EC-5 sensors is shown in the lower plot. Red dots and error bars show the averaged Time Domain Reflectometry measurements at 4 dates (black crosses in Figure 1c).

3.2. Simulation of Neutron Transport

3.2.1. Leerodt Field

Neutron counts of the three CRNS in the Leerodt field and their corresponding URANOS simulations are shown in Figure 5. The URANOS simulations were performed using the Leerodt domain, which is based on land use, BK5, and EMI maps. Details on the creation of this domain are provided in Appendix B.

In Figure 5, the three panels on the left illustrate the effect of a 30 mm precipitation event on 23rd June 2023. In this case, URANOS simulations closely matched the measurements for CRNS-1 but slightly overestimated neutron count rates for CRNS-2 and CRNS-3. Overall, the agreement is satisfactory, considering the simplifications in the URANOS simulations and the smoothing applied to CRNS readings.

The right panels in Figure 5 show a 15-day period in July 2023 when irrigation and precipitation co-occurred. In the figure, the color of each CRNS matches that of irrigation in the line where a CRNS was installed, while light gray shows irrigation in line L-0, where no CRNS was present. The first irrigation occurred on 7th July in line L-0 and is closely preceded by 6 mm precipitation. Given such complexity and distance from the CRNS, a comparison between URANOS simulations and the CRNS signals was not possible. Following a 22 and 8 mm rainfall on 9th and 12th July, respectively, a modest 14 mm irrigation in line L-1 had little effect on CRNS-1, despite agreement between simulated and measured counts after irrigation. Similarly, CRNS-2 showed no response and measured counts were lower than simulated, likely due to prior precipitation and the small irrigation volume, which the URANOS scenarios of this work did not fully account for. On 14th July, 27 mm of irrigation in line L-2 produced good agreement between simulations and measurements at CRNS-2, despite prior rainfall. For CRNS-3, however, URANOS overestimated the effect of nearby irrigation, as measured counts remained stable. Finally, irrigation in line L-3 on 16th July resulted in good agreement at CRNS-3, but for nearby CRNS-2, measured counts increased faster than predicted by simulations. Overall, the two-tube CRNS-2 appeared more sensitive than the other sensors to both precipitation and irrigation. It also better matched URANOS simulations of irrigation. This is likely due to its higher count rate and central position and suggests that instruments with higher count rates and central placement within the field may more effectively monitor irrigation under complex environmental conditions.

The influence of nearby irrigation on neutron detection is further analyzed in Figure 6, which shows the neutron contribution from the irrigation lines and from outside the field in dry conditions. For all three CRNS, the majority

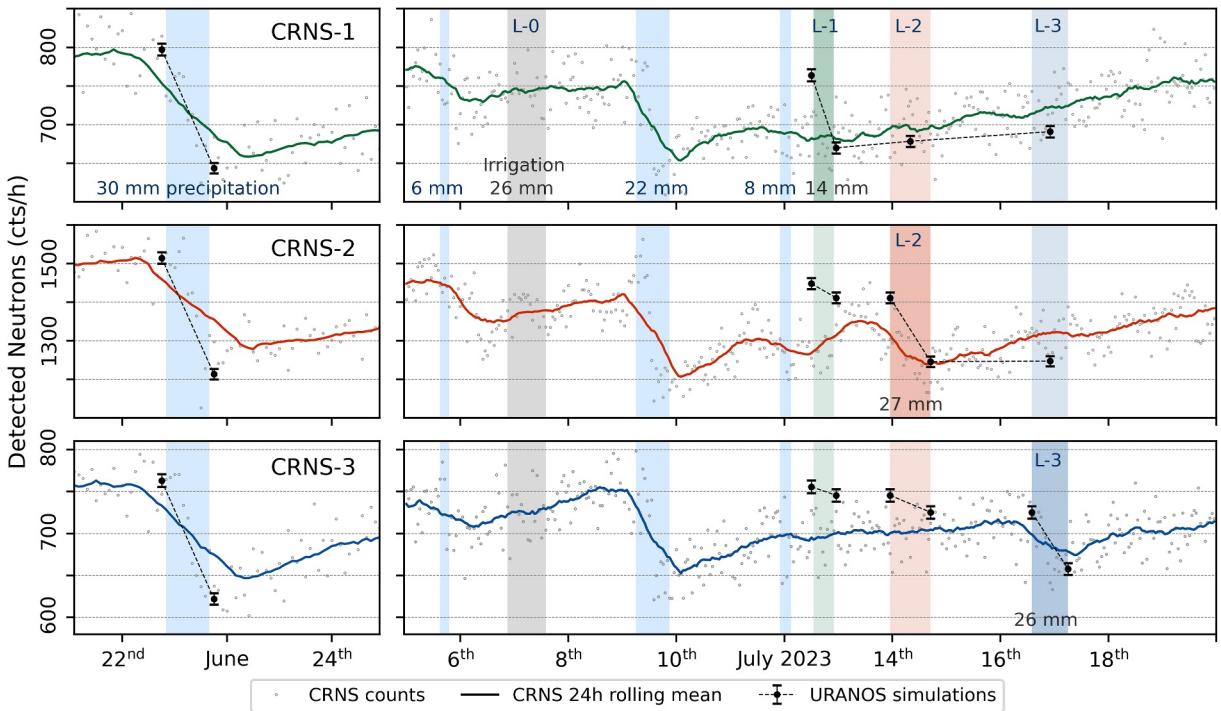

Figure 5. Measured neutron counts of the three Cosmic-ray neutron sensors with corrected hourly values (gray dots), and 24-hr rolling means (colored lines). Black dots and error bars show the values simulated with URANOS. Dashed black lines show the simulated change in detection before and after a specific precipitation or irrigation event. Left panels show the effect of a precipitation event on 23rd June 2023 while right panel shows the effects of the consecutive irrigation of the four irrigation lines mixed with precipitation. As in Figure 2, precipitation events are indicated with light blue areas and irrigation is shown by areas colored according to the irrigation line: gray for L-0, green for L-1 (where CRNS-1 is located), orange for L-2 (CRNS-2), and blue for L-3 (CRNS-3).

(around 60%) of detected neutrons originate in the irrigation line where the sensor is installed. The other irrigation lines provide much lower contributions: around 11%–14% if the line is approximately 20 m from the CRNS and around 4%–6% if the line is approximately 50 m away.

Next, URANOS results were compared with the analytical approach of Schrön et al. (2023), with results provided in Table 3. This table shows the change of neutron counts following the irrigation and drying scenarios outlined in Section 2.5.1. A positive change ("+") indicates a percentage increase of neutrons due to drying, while "–" indicates a decrease due to nearby irrigation. The comparison is shown for the three different CRNS stations (rows) and for subsequent irrigation events occurring in the four different irrigation lines L-0 to L-3 (see notations in Figures 1a and 6). For example, irrigation of L-3 reduces neutron counts of the most nearby sensor CRNS-3, while at the same time, the neutrons of sensors CRNS-1 and CRNS-2 decrease. This is because the drying out of the nearby lines has stronger effect on those sensors than the irrigation of the remote line.

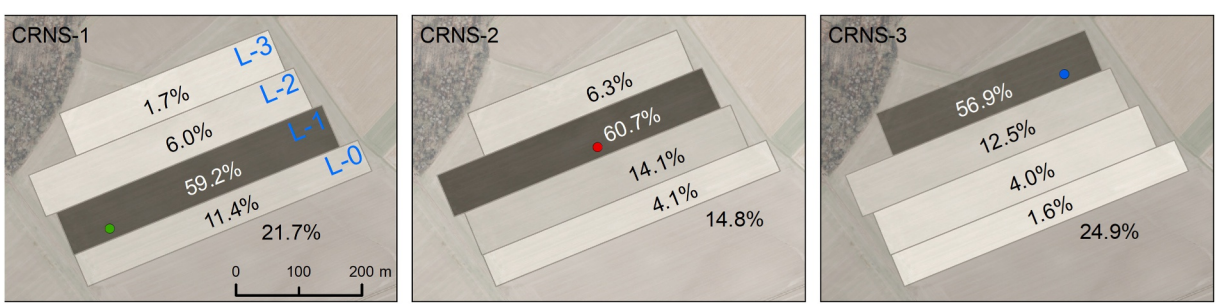

Figure 6. Contribution to simulated signal of the irrigation lines and of the surrounding area for CRNS-1 (left panel), CRNS-2 (central panel), and CRNS-3 (right panel). Contributions are calculated for the dry scenario in URANOS and shown as percentage of neutrons that have first soil contact in each area.

Table 3
Calculated Variations (in %) of Detected Neutrons Caused by Consecutive Irrigation and Drying Events (Described in Section 2.5.1) at the Four Irrigated Lines (L-0 to L-3 in Figures 1a and 6) Using Two Different Methods: The URANOS Simulations Model and the Analytical Estimation of Schrön et al. (2023)

CRNS	Method	L-0	L-1	L-2	L-3
CRNS-3	URANOS Simulations	+0.1%	−1.4%	−2.7%	−9.3%
	Analytical Solution	−0.2%	−0.5%	−1.8%	−11.2%
CRNS-2	URANOS Simulations	−0.6%	−2.5%	−11.7%	+0.1%
	Analytical Solution	−0.6%	−2.2%	−11.8%	+1.2%
CRNS-1	URANOS Simulations	−1.5%	−12.3%	+1.3%	+1.8%
	Analytical Solution	−2.1%	−11.1%	+1.0%	+1.5%

Note. SWC changes until 30 cm depth are considered in the analytical solution results. For both approaches, a relative error of approximately 1% should be taken into consideration.

Overall, the changes in neutron counts estimated by the analytical solution closely matched the URANOS simulations, especially considering the general uncertainty of the URANOS results (approx. 1%) and the soil homogeneity assumptions of the analytical approach. Only in the case of CRNS-3 and irrigation in line L-3 the discrepancy was noticeable: −9.3% for URANOS simulations and −11.2% for the analytical solution. This agreement with URANOS in a complex environment, such as irrigation of different lines, demonstrates that the analytical solution, despite its simplified nature, is a relatively rapid and precise approach with potential for application in complex scenarios. However, it should be noted that only a soil depth of 30 cm was considered, which corresponds to the first soil layer in the URANOS domain. Considering deeper soils requires an integration of SWC variations as the current version of the analytical tool only considers one homogeneous soil layer. Additional depths of 50 and 80 cm were analyzed and generally resulted in underestimations of irrigation effects compared to URANOS simulations (see Appendix C). This suggests that, despite the good results of this study, the analytical solution of Schrön et al. (2023) could benefit from including vertical heterogeneity in SWC, particularly for small-scale irrigation studies.

Overall, Figures 5 and 6, and Table 3 demonstrate that URANOS could reproduce the effects of precipitation and of certain irrigation events at the respective CRNS locations. However, some variations in observed neutron counts were not fully captured, as preceding and subsequent precipitation events introduced spatio-temporal complexities in SWC patterns beyond the scope of the URANOS simulations. Small, simulated variations due to irrigation in nearby lines were, in general, not observed. Many of these simulated changes were minor and within the simulation's relative errors, making them difficult to detect under the conditions of the observation period. In addition, the URANOS simulations considered an irrigation that rapidly changes the SWC on a given line, while the irrigation generally took half a day or more due to the slow speed and flow of the hose reel raingun. Moreover, since CRNS is known to have a much lower uncertainty and a higher sensitivity under very dry conditions (below 0.15 $m^3\ m^{-3}$) the small simulated SWC variations could possibly be visible in dryer periods or in more arid sites. Nevertheless, the measurement accuracy of the CRNS detectors used in this study was not sufficient to detect most irrigation events occurring in the nearby lines. The use of detectors with higher sensitivity may have resulted in smaller uncertainties and allowed the use of shorter integration times, thus reducing uncertainty and rendering small SWC variations detectable.

3.2.2. Oehna Field

The results of URANOS simulations of the Oehna field are shown in Figure 7 alongside measured counts for the period from 16th May to 28th June 2023. During this time, five irrigation events occurred, along with two small rainfalls of 6 and 5 mm. After the irrigation period, a large precipitation event occurred on 23rd–24th June. This precipitation event and the last irrigation on 17th June were well captured by URANOS, with simulated neutron

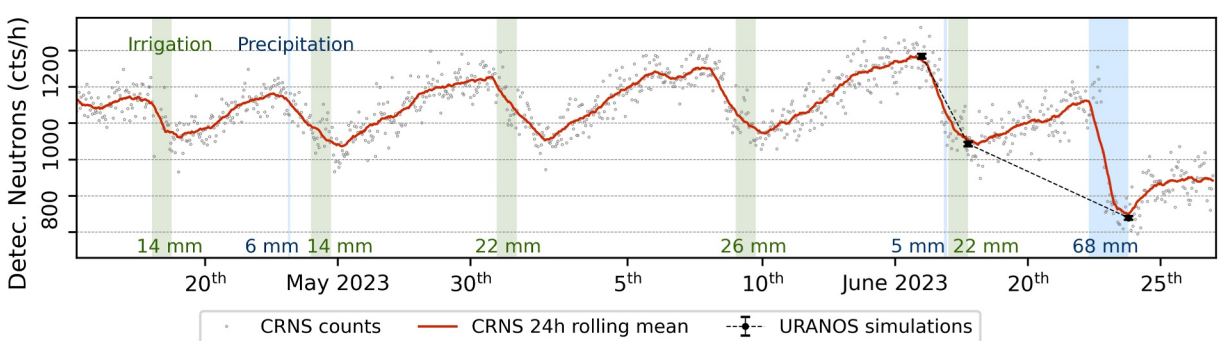

Figure 7. Measured neutron counts in Oehna with corrected hourly values (gray dots) and 24-hr rolling mean (red line). Black dots and error bars show the values simulated with URANOS.

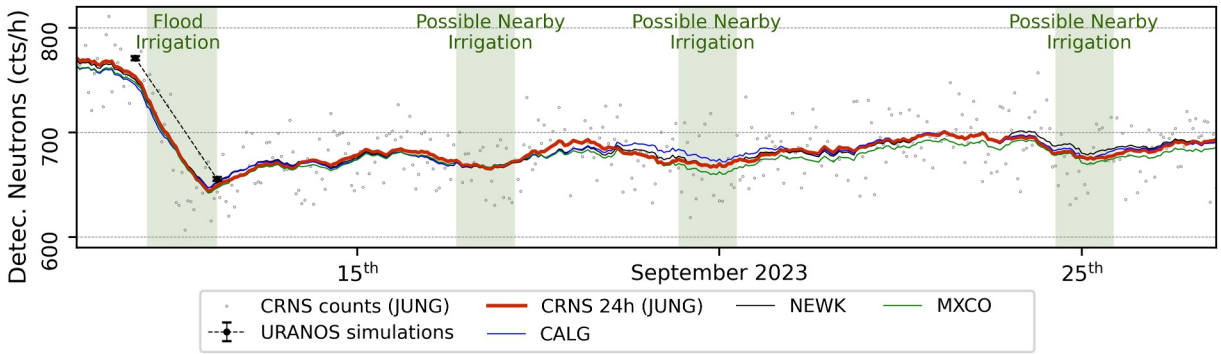

Figure 8. Measured neutron counts in Davis with corrected hourly values (gray dots) and 24 hr rolling mean (lines) using four different neutron monitors. Black dots and error bars show the values simulated with URANOS.

counts closely matching the observations. The relative simplicity of the investigated site also contributed to the accuracy of the simulation as the Oehna field is relatively large and the irrigation area covers the CRNS footprint. Overall, the results indicate that URANOS can reliably reproduce irrigation and rainfall dynamics in this field.

3.2.3. Davis Field

Figure 8 shows neutron counts measured in the Davis field together with URANOS-simulated counts for the period 10th–18th September 2023. The flood irrigation on 12th September was well reproduced by the simulations. Later in the month, possible irrigation of a large field located about 100 m from the CRNS appears to coincide with drops in the neutron counts on the 17th, 20th, and 25th September. According to URANOS simulations, for this area and instrumentation, this irrigation can only result in changes below 1% of the neutron count. While the drops shown in Figure 8 may be coherent with such changes, they are still relatively small and the URANOS simulations had a relative error of approximately 0.5%. Thus, it cannot be excluded that the observed drops in neutron counts originate from other sources such as limitations in the corrections that were applied or water spilling from the nearby fields into the investigated field. To partially exclude the influence of the incoming correction, neutron counts were additionally corrected by using neutron monitors in Calgary (CALG), Mexico City (MXCO) and Newark (NEWK). The results of using these neutron monitors are shown in different colors in Figure 8. Overall, for this period, limited differences emerged from using these alternative neutron monitors and the small drops in neutron counts remained noticeable. Although these small variations cannot be clearly attributed to nearby irrigation, URANOS accurately reproduced the direct effects of flood irrigation in the Davis field and proved valuable for interpreting CRNS signals and investigating small events beyond the reach of point-scale sensors.

3.3. Limitations of This Study and Perspectives for Researchers and Stakeholders

This study combined extensive field measurements and neutron transport simulations that provided valuable insights, yet certain limitations must be acknowledged. The URANOS simulations proved useful for reproducing observations, but they remain a simplification of real conditions, with simplified vegetation and, in Leerodt, a relatively low resolution of 10 m. In the Leerodt experiment, reproducing the full sequence of rainfall and irrigation events was not feasible, as it would have required an impractically large number of simulations. In addition, soil erosion frequently affected the profile sensors and periodic reinstallation was not possible. Future studies could mitigate such effects by installing sensors at greater depths and revisiting measurement sites more regularly. Finally, some of the point-scale instruments used generalized or factory-provided calibrations. While this may have slightly reduced the quality of the SWC readings, especially for the FDR sensors, this did not affect the conclusions of this study.

Results from the Leerodt experiment (hose reel raingun irrigation) showed that CRNS may fail to detect nearby irrigation and, in extreme cases, even irrigation at the sensor location, particularly when precipitation co-occurred. This may seem inconsistent with current knowledge on CRNS; however, most studies to date have focussed on responses to natural events, such as rainfall. Irrigation presents fundamental differences, as it is generally more susceptible to runoff and evaporation and primarily affects the topsoil, whereas CRNS integrates over deeper

layers, particularly under dry conditions. Some studies emphasized the role of vertical soil moisture profiles (Baroni et al., 2018; Brogi et al., 2022; Scheiffele et al., 2020; Schrön et al., 2017). However, most research tends to consider SWC heterogeneity within the CRNS footprint as a two-dimensional problem (Brogi et al., 2023; Rasche et al., 2021; Schrön et al., 2023). Therefore, the findings of the present study suggest that a more three-dimensional interpretation of SWC variations within the CRNS sensing volume is better suited to explain certain irrigation effects. In addition, in cases where the volume of soil that is affected by irrigation is relatively small compared to the CRNS footprint, future studies could perform comparisons not only of CRNS and point-scale sensors, but also of other intermediate-scale methods such as Gamma-Ray spectroscopy (Akter et al., 2025; Filippucci et al., 2020; Scudiero et al., 2024; Serafini et al., 2021; Strati et al., 2018), which estimates SWC over a smaller area compared to CRNS.

CRNS responses were more pronounced under flood and pivot irrigation, but dampened or masked under hose reel raingun, particularly when precipitation and irrigation occurred simultaneously. Thus, although CRNS shows potential for irrigation monitoring, it cannot yet be considered consistently effective for irrigation systems that moisten only a small soil volume within the footprint. This does not imply that, in complex settings, CRNS offers no advantages for sustainable irrigation practices, where the aim is to maximize yields by optimizing water applications and root water uptake. CRNS remain well suited to monitor field-scale water availability in the rootzone and, in irrigation systems affecting only a small soil volume (e.g., drip irrigation), it can assess the long-term effectiveness of irrigation rather than monitor localized SWC variations, while point-scale sensors are used to capture short-term localized effects. For example, if CRNS-derived SWC decreases over several days while point sensors near irrigation outlets measure consistently high values, it indicates insufficient root-zone wetting across the field, insufficient irrigation, and potential crop water stress despite seemingly favorable point-scale readings.

Finally, the potential of CRNS for operational irrigation management is not yet fully developed, which is partly due to the method's technical complexity. While recent and upcoming developments such as the Neptoon Python tool (Power et al., 2025) and community-agreed standards will likely simplify CRNS use, broader CRNS adoption will require additional support. In the authors' view, instrument manufacturers could play a decisive role by further collaborating with the scientific community to extend their focus and integrating tools like a) URANOS (Köhli et al., 2023), b) the simpler analytical approach of Schrön et al. (2023), c) the versatile Virtual Joint Field Campaign framework (Francke et al., 2025), or d) the small-field correction proposed by Brogi et al. (2023). These tools can predict CRNS performance before installation, guide sensor selection and placement, improve data interpretation, and ultimately enhance the transferability of the method across irrigation systems. However, these methods are complex and may hamper easy implementation of CRNS systems for farming applications. From this perspective, a stronger collaboration between industry and research may be useful. If manufacturers would invest in this direction, even with simplified and instrument-specific tools, they could provide farmers with SWC estimates representative of the target irrigated field rather than of the entire CRNS footprint. Additionally, pilot test fields where irrigation is optimized trough instrumentation and modeling could be used to a) assess and streamline both CRNS and its irrigation correction methods and b) directly showcase the advantages to stakeholders. This would increase the potential economic return for the farmer and thus the value of a CRNS device. Ideally, this would be followed by the integration of CRNS into irrigation management services that combine measurements and process-based or data-driven modeling approaches that can provide farmers with clear, easily actionable recommendations for efficient irrigation scheduling.

4. Conclusions

This study evaluated CRNS performance under three irrigation systems: hose reel raingun (potato), central pivot sprinklers (winter wheat), and flood irrigation (alfalfa). Compared to point-scale and profile sensors, CRNS provided SWC estimates that more accurately represented field-scale dynamics and were less affected by local disturbances such as soil erosion. Soil erosion was particularly detrimental to profile sensors, resulting in unrealistic readings that occasionally reached 0 cm^3 cm^{-3} in the hose reel raingun irrigated field. CRNS effectiveness in irrigation monitoring strongly depended on irrigation type. Flood irrigation produced clear responses, while central pivot yielded somewhat dampened signals due to the greater depth over which CRNS integrates SWC. Under hose reel raingun, where only a small portion of the footprint was wetted, CRNS responses were sometimes weak or even absent, especially for sensors with lower count rates. The UTS approach improved SWC

estimation at low water contents (below 0.10 cm^3 cm^{-3}), avoiding the unrealistically low values sometimes produced by the N0 approach, while both approaches agreed well at SWC values between 0.10 and 0.40 cm^3 cm^{-3}.

Neutron transport simulations with the URANOS model, despite the relatively simplified representation of the modeling domain, reproduced field observations well under flood and pivot irrigation. For the moving sprinkler system, simulations captured precipitation effects but did not fully reproduce irrigation impacts, primarily due to the co-occurrence of precipitation and to the relatively small variations in simulated neutron counts (1%–2%, which is close to the simulation uncertainty). Despite this, simulations provided valuable support for interpreting and assessing measurements. A simpler analytical solution produced comparable results and is promising for rapid applications, although its assumption of vertically homogeneous soils currently limits accuracy when SWC changes are confined to shallow layers.

Overall, combining neutron transport simulations and CRNS measurements can greatly improve the interpretation of CRNS observations across irrigation systems. In addition, CRNS performance is influenced by irrigation type and site-specific conditions, highlighting the need for site-specific interpretation. Wider adoption of CRNS would benefit if manufacturers increasingly integrated neutron transport modeling tools and recent methodological advances into their systems. This would enable both researchers and other stakeholders such as farmers to make informed decisions before CRNS deployment and to obtain SWC estimates that better reflect their site-specific irrigation setups and needs.

Appendix A: Loss of Soil Contact of Profile Point-Scale Sensors

Figure A1 shows the conditions of profile point-scale sensors in the Leerodt field on 20 September 2023. The loss of soil contact due to erosion of the soil ridges is apparent. Moreover, the dislocation of soil from the ridge to the alleys has modified the depth of the sensor as its top is not leveled with the soil surface like at the time of installation.

Figure A1. Picture of a SoilVUE10 sensor in the Leerodt field showing loss of soil contact due to soil erosion.

Appendix B: Generation of URANOS Domain for Leerodt Field

Figure B1 shows some steps of the generation of the URANOS domain for the Leerodt field. The left map shows one of the nine measured ECa maps obtained by using the 3-coil CMD-MiniExplorer in vertical coplanar (VCP) configuration and the 6-coil CMD-MiniExplorer Special-Edition horizontal coplanar (HCP) configuration. The resulting DOI ranged from 0 to 89 cm for the 3-coil device and from 0 to 270 cm for the 6-coil device (McNeill, 1980). Both EMI instruments were equipped with a DGPS (Trimble Inc, Westmister CO, USA) and positioned inside custom-made plastic sleds. These sleds were pulled by an all-terrain vehicle at a speed of 5–8 km/h along parallel lines, generally separated by 10 m distance. The 5 Hz measurement frequency resulted in an

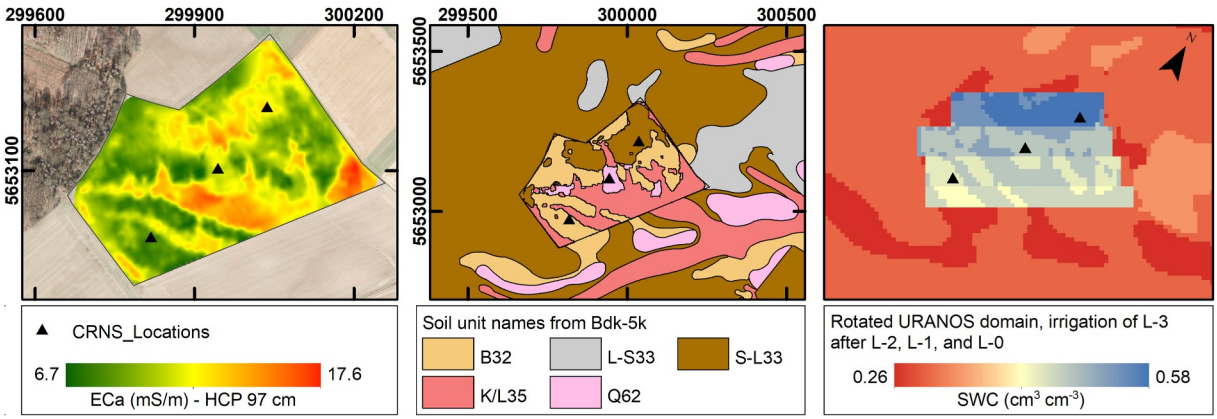

Figure B1. Generation of the URANOS domain for the Leerodt field: the left panel shows an ECa map of the investigated field (depths of investigation = 0–145 cm), the central panel shows a soil map combining ECa-based classification and Bk5 map soil units, and the right panel shows the distribution of soil water content in the first 30 cm of soil for a portion of the rotated domain (scenario with consecutive wetting of the four irrigation lines inside the field).

in-line resolution of 35–45 cm. Measured ECa data was filtered to remove outliers using a min-max filter, a histogram filter, and a variation threshold filter (Brogi et al., 2019; von Hebel et al., 2014). Finally, interpolated ECa maps with 2.5 m resolution were obtained by applying a Kriging approach with Gaussian semivariogram using ArcGIS version 10.7.1. The central map in Figure B 1 shows the soil map obtained by combining the classified EMI map with the local soil map. The right panel shows an example of the 10 m resolution domain after rotation and with SWC distribution in the first 30 cm of soil (after irrigation in the four lines L-0 to L-3).

Appendix C: Effect of Considering Different Soil Depths With the Distant Area Analytical Tool

Table C1, similarly to Table 3, shows the simulated variation in detected neutrons due to irrigation and dry out as estimated by URANOS simulations and by the analytical solution of Schrön et al. (2023). For the analytical solution, soil depths of 30, 50, and 80 cm are considered. The analytical solution considers a homogeneous soil layers and, for 30 cm depth, the initial SWC values and the SWC variations were the same as in the first soil layer of the URANOS simulations. If deeper soils are considered, initial SWC conditions and SWC variations must be

Table C1
Similarly to Table 3, Calculated Variations (in %) of Detected Neutrons Caused by Consecutive Irrigation and Drying Events (Described in Section 5.2.1) Occurring on the Four Field Irrigated Lines (L-0 to L-3 in Figures 1a and 6) Using Two Different Methods: The URANOS Simulations Model and the Analytical Estimation of Schrön et al. (2023). For the URANOS Simulations, a Relative Error of Approximately 1% Should be Taken Into Consideration

CRNS	Method	L-0	L-1	L-2	L-3
CRNS-3	URANOS Simulations	+0.1%	−1.4%	−2.7%	−9.3%
	Analytical 30 cm	−0.2%	−0.5%	−1.8%	−11.2%
	Analytical 50 cm	−0.2%	−0.4%	−1.4%	−8.1%
	Analytical 80 cm	−0.1%	−0.2%	−0.9%	−4.5%
CRNS-2	URANOS Simulations	−0.6%	−2.5%	−11.7%	+0.1%
	Analytical 30 cm	−0.6%	−2.2%	−11.8%	+1.2%
	Analytical 50 cm	−0.5%	−1.6%	−8.7%	+0.7%
	Analytical 80 cm	−0.3%	−1.0%	−5.9%	+0.5%
CRNS-1	URANOS Simulations	−1.5%	−12.3%	+1.3%	+1.8%
	Analytical 30 cm	−2.1%	−11.1%	+1.0%	+1.5%
	Analytical 50 cm	−1.5%	−8.0%	+0.6%	+1.0%
	Analytical 80 cm	−1.1%	−5.2%	+0.4%	+0.7%

integrated over multiple soil layers. In the case of the Leerodt field, this resulted in a) generally higher initial SWC conditions and b) lower SWC variations due to irrigation. Irrigation in the Leerodt field mostly affected shallow SWC and deeper soils generally had higher SWC than shallow soils. The consequence is that the SWC variations fed to the analytical solution are smaller for 50 cm and even smaller for 80 cm, resulting in underestimations compared to the URANOS simulations where multiple soil depths were considered.

Conflict of Interest

The authors declare no conflicts of interest relevant to this study.

Availability Statement

Measured data, simulations blueprints and results, and materials to reproduce figures and maps of this study can be downloaded here: https://data.fz-juelich.de/dataset.xhtml?persistentId=doi:10.26165/JUELICH-DATA/YYCOTH.

Acknowledgments
Support was received from the Deutsche Forschungsgemeinschaft (DFG, German Research Foundation) project 357874777 of the research unit FOR 2694 Cosmic Sense, from the BMBF BioökonomieREVIER funding scheme with its "BioRevierPlus" project "DG-RR" (Grant 031B1137D/031B1137DX), from Germany's Excellence Strategy EXC 2070, Grant 390732324—PhenoRob, and from USDA NIFA (Award # 2021–68012–35914). We thank Markus Köhli (Physikalisches Institut, Heidelberg University, Germany, and CEO at Styx Neutronica GmbH) for his consistent work on URANOS and thank the team that develops and allows the use of this model. For the Leerodt site, we thank Simon Keutmann and Marco Breuer from the Chamber of Agriculture North Rhine-Westphalia and Andrian Gehring for the help during instrument installations, maintenance, and calibration. We thank Willi Jäger for granting access to the Leerodt field and for his general support of the investigation. We thank Sophia Scheibel and Salar Saeed Dogar for their help with geophysical measurements. For the Oehna site, we thank Adane Buni Irkiso and María Olivia García Quiroz for calibration sampling and sample handling, carried out as part of their theses. For the Davis field, we thank Mark Rubio, the farm manager at UCD, for his support and we thank visiting scholar Francisco Puig for field data collection.We also thank Daniel Rasche (GFZ Helmholtz Centre for Geosciences, Potsdam, Germany) for providing the response function of a Helium-3 proportional counter tube with 25 mm high density polyethylene (HDPE) moderator and Marcello Lunardon (University of Padua, Padua, Italy) for providing the response function of a Finapp3 with 15 mm HDPE moderator. Open Access funding enabled and organized by Projekt DEAL.

References

Abioye, E. A., Abidin, M. S. Z., Mahmud, M. S. A., Buyamin, S., Ishak, M. H. I., Abd Rahman, M. K. I., et al. (2020). A review on monitoring and advanced control strategies for precision irrigation. *Computers and Electronics in Agriculture*, *173*, 105441. https://doi.org/10.1016/j.compag.2020.105441

Adeyemi, O., Grove, I., Peets, S., Domun, Y., & Norton, T. (2018). Dynamic neural network modelling of soil moisture content for predictive irrigation scheduling. *Sensors*, *18*(10), 3408. https://doi.org/10.3390/s18103408

Adeyemi, O., Grove, I., Peets, S., & Norton, T. (2017). Advanced monitoring and management systems for improving sustainability in precision irrigation. *Sustainability*, *9*(3), 353. https://doi.org/10.3390/su9030353

Akter, S., Huisman, J. A., & Bogena, H. R. (2025). Comparing the accuracy of soil moisture estimates derived from bulk and energy-resolved gamma radiation measurements. *Sensors*, *25*(14), 4453. https://doi.org/10.3390/s25144453

Andreasen, M., Jensen, K. H., Desilets, D., Zreda, M., Bogena, H. R., & Looms, M. C. (2017). Cosmic-ray neutron transport at a forest field site: The sensitivity to various environmental conditions with focus on biomass and canopy interception. *Hydrology and Earth System Sciences*, *21*(4), 1875–1894. https://doi.org/10.5194/hess-21-1875-2017

Andreasen, M., Kragh, S. J., Meyer, R., Jensen, K. H., & Looms, M. C. (2023). Mapping spatiotemporal soil moisture in highly heterogeneous agricultural landscapes using mobile dual-spectra cosmic-ray neutron sensing. *Vadose Zone Journal*, *22*(6), e20287. https://doi.org/10.1002/vzj2.20287

Andreasen, M. J., K, H., Desilets, D., Franz, T. E., Zreda, M., Bogena, H. R., & Looms, M. C. (2017). Status and perspectives on the cosmic-ray neutron method for soil moisture estimation and other environmental science applications. *Vadose Zone Journal*, *16*(8), 1–11. https://doi.org/10.2136/vzj2017.04.0086

Arnault, J., Benjamin, F., Schrön, M., Bogena, H. R., Hendricks Franssen, H. J., & Kinstmann, H. (2024). Role of infiltration on land–atmosphere feedbacks in Central Europe: Fully coupled WRF-Hydro simulations evaluated with cosmic-ray neutron soil moisture measurements. In *Journal of Hydrometeorology*. Accepted for publication. https://doi.org/10.1175/JHM-D-24-0049.1

Baatz, R., Hendricks Franssen, H.-J., Han, X., Hoar, T., Bogena, H. R., & Vereecken, H. (2017). Evaluating the value of a network of cosmic-ray probes for improving land surface modeling. *Hydrology and Earth System Sciences*, *21*, 2509–2530. https://doi.org/10.5194/hess-2016-432

Babaeian, E., Sadeghi, M., Franz, T. E., Jones, S., & Tuller, M. (2018). Mapping soil moisture with the OPtical TRApezoid Model (OPTRAM) based on long-term MODIS observations. *Remote Sensing of Environment*, *211*, 425–440. https://doi.org/10.1016/j.rse.2018.04.029

Bangash, R. F., Passuello, A., Sanchez-Canales, M., Terrado, M., López, A., Elorza, F. J., et al. (2013). Ecosystem services in Mediterranean river basin: Climate change impact on water provisioning and erosion control. *Science of the Total Environment*, *458*, 246–255. https://doi.org/10.1016/j.scitotenv.2013.04.025

Barker, J. B., Franz, T. E., Heeren, D. M., Neale, C. M., & Luck, J. D. (2017). Soil water content monitoring for irrigation management: A geostatistical analysis. *Agricultural Water Management*, *188*, 36–49. https://doi.org/10.1016/j.agwat.2017.03.024

Baroni, G., Scheiffele, L. M., Schrön, M., Ingwersen, J., & Oswald, S. E. (2018). Uncertainty, sensitivity and improvements in soil moisture estimation with cosmic-ray neutron sensing. *Journal of Hydrology*, *564*, 873–887. https://doi.org/10.1016/j.jhydrol.2018.07.053

Bogena, H., Huisman, J., Güntner, A., Hübner, C., Kusche, J., Jonard, F., et al. (2015). Emerging methods for noninvasive sensing of soil moisture dynamics from field to catchment scale: A review. *Wiley Interdisciplinary Reviews. Water*, *2*(6), 635–647. https://doi.org/10.1002/wat2.1097

Bogena, H., Schrön, M., Jakobi, J., Ney, P., Zacharias, S., Andreasen, M., et al. (2022). COSMOS-Europe: A European network of cosmic-ray Neutron soil moisture sensors. *Earth System Science Data Discussions*, *14*(3), 1–33. https://doi.org/10.5194/essd-14-1125-2022

Bogena, H. R., Herbst, M., Huisman, J. A., Rosenbaum, U., Weuthen, A., & Vereecken, H. (2010). Potential of wireless sensor networks for measuring soil water content variability. *Vadose Zone Journal*, *9*(4), 1002–1013. https://doi.org/10.2136/vzj2009.0173

Bogena, H. R., Herrmann, F., Jakobi, J., Brogi, C., Ilias, A., Huisman, J. A., et al. (2020). Monitoring of snowpack dynamics with cosmic-ray neutron probes: A comparison of four conversion methods. *Frontiers in Water*, *2*, 19. https://doi.org/10.3389/frwa.2020.00019

Brogi, C., Bogena, H. R., Köhli, M., Huisman, J. A., Hendricks Franssen, H.-J., & Dombrowski, O. (2022). Feasibility of irrigation monitoring with cosmic-ray neutron sensors. *Geosci. Instrum. Method. Data Syst.*, *11*(2), 451–469. https://doi.org/10.5194/gi-11-451-2022

Brogi, C., Huisman, J. A., Pätzold, S., von Hebel, C., Weihermüller, L., Kaufmann, M. S., et al. (2019). Large-scale soil mapping using multi-configuration EMI and supervised image classification. *Geoderma*, *335*, 133–148. https://doi.org/10.1016/j.geoderma.2018.08.001

Brogi, C., Jakobi, J., Huisman, J., Schmidt, M., Montzka, C., Bates, J., et al. (2025). Cosmic-ray neutron sensors provide scale-appropriate soil water content and vegetation observations for eddy covariance stations in agricultural ecosystems. *Agricultural and Forest Meteorology*, *373*, 110731. https://doi.org/10.1016/j.agrformet.2025.110731

Brogi, C., Pisinaras, V., Köhli, M., Dombrowski, O., Hendricks Franssen, H., Babakos, K., et al. (2023). Monitoring irrigation in small orchards with cosmic-ray neutron sensors. *Sensors*, *23*(5), 2378. https://doi.org/10.3390/s23052378

Chartzoulakis, K., & Bertaki, M. (2015). Sustainable water management in agriculture under climate change. *Agriculture and Agricultural Science Procedia*, *4*, 88–98. https://doi.org/10.1016/j.aaspro.2015.03.011

Chathuranika, I., Khaniya, B., Neupane, K., Rustamjonovich, K. M., & Rathnayake, U. (2022). Implementation of water-saving agro-technologies and irrigation methods in agriculture of Uzbekistan on a large scale as an urgent issue. *Sustainable Water Resources Management*, *8*(5), 155. https://doi.org/10.1007/s40899-022-00746-6

Chen, X., Song, W., Shi, Y., Liu, W., Lu, Y., Pang, Z., & Chen, X. (2022). Application of cosmic-ray Neutron sensor method to calculate field water use efficiency. *Water*, *14*(9), 1518. https://doi.org/10.3390/w14091518

Corwin, D. L., & Lesch, S. M. (2003). Application of soil electrical conductivity to precision agriculture. *Agronomy Journal*, *95*(3), 455–471. https://doi.org/10.2134/agronj2003.4550

Desilets, D., & Zreda, M. (2003). Spatial and temporal distribution of secondary cosmic-ray nucleon intensities and applications to in situ cosmogenic dating. *Earth and Planetary Science Letters*, *206*(1–2), 21–42. https://doi.org/10.1016/S0012-821X(02)01088-9

Desilets, D., Zreda, M., & Ferré, T. P. A. (2010). Nature's neutron probe: Land surface hydrology at an elusive scale with cosmic rays. *Water Resources Research*, *46*(11). https://doi.org/10.1029/2009WR008726

Dombrowski, O., Brogi, C., Hendricks Franssen, H. J., Pisinaras, V., Panagopoulos, A., Swenson, S., & Bogena, H. (2024). Land surface modeling as a tool to explore sustainable irrigation practices in Mediterranean fruit orchards. *Water Resources Research*, *60*(7), e2023WR036139. https://doi.org/10.1029/2023WR036139

Dong, J., & Ochsner, T. E. (2018). Soil texture often exerts a stronger influence than precipitation on mesoscale soil moisture patterns. *Water Resources Research*, *54*(3), 2199–2211. https://doi.org/10.1002/2017WR021692

Elliott, J., Deryng, D., Müller, C., Frieler, K., Konzmann, M., Gerten, D., et al. (2014). Constraints and potentials of future irrigation water availability on agricultural production under climate change. *Proceedings of the National Academy of Sciences*, *111*(9), 3239–3244. https://doi.org/10.1073/pnas.1222474110

ESRI. (2025). DIgitalGlobe, GeoEye, earthstar geographics, CNES/Airbus DS, USDA, AEX, getmapping, Aerogrid, IGN, IGP, swisstopo, and the GIS user comunity.

European Commission: Directorate-General for Research and Innovation and Group of Chief Scientific Advisors. (2020). *Towards a sustainable food system—Moving from food as a commodity to food as more of a common good—Independent expert report*. Publications Office. Retrieved from https://data.europa.eu/doi/10.2777/282386

Evans, R. G., & Sadler, E. J. (2008). Methods and technologies to improve efficiency of water use. *Water Resources Research*, *44*(7). https://doi.org/10.1029/2007WR006200

Evett, S. R., Schwartz, R. C., Tolk, J. A., & Howell, T. A. (2009). Soil profile water content determination: Spatiotemporal variability of electromagnetic and neutron probe sensors in access tubes. *Vadose Zone Journal*, *8*(4), 926–941. https://doi.org/10.2136/vzj2008.0146

FAO. (2022). *World food and agriculture-statistical pocketbook. Food & agriculture Organization of the UN*. FAO.

Filippucci, P., Tarpanelli, A., Massari, C., Serafini, A., Strati, V., Alberi, M., et al. (2020). Soil moisture as a potential variable for tracking and quantifying irrigation: A case study with proximal gamma-ray spectroscopy data. *Advances in Water Resources*, *136*, 103502. https://doi.org/10.1016/j.advwatres.2019.103502

Finkenbiner, C. E., Franz, T. E., Gibson, J., Heeren, D. M., & Luck, J. (2019). Integration of hydrogeophysical datasets and empirical orthogonal functions for improved irrigation water management. *Precision Agriculture*, *20*(1), 78–100. https://doi.org/10.1007/s11119-018-9582-5

Francke, T., Brogi, C., Duarte Rocha, A., Förster, M., Heistermann, M., Köhli, M., et al. (2025). Virtual Joint Field Campaign: A framework of synthetic landscapes to assess multiscale measurement methods of water storage. *Geoscientific Model Development*, *18*(3), 819–842. https://doi.org/10.5194/gmd-18-819-2025

Franz, T., Wahbi, A., Vreugdenhil, M., Weltin, G., Heng, L., Oismueller, M., et al. (2016). Using cosmic-ray neutron probes to monitor landscape scale soil water content in mixed land use agricultural systems. *Applied and Environmental Soil Science*, *2016*, 1–11. https://doi.org/10.1155/2016/4323742

Franz, T. E., Wahbi, A., Zhang, J., Vreugdenhil, M., Heng, L., Dercon, G., et al. (2020). Practical data products from cosmic-ray neutron sensing for hydrological applications. *Frontiers in Water*, *2*, 9. https://doi.org/10.3389/frwa.2020.00009

Franz, T. E., Zreda, M., Rosolem, R., & Ferre, T. P. A. (2012). Field validation of a cosmic-ray neutron sensor using a distributed sensor network. *Vadose Zone Journal*, *11*(4), vzj2012–vzj2046. https://doi.org/10.2136/vzj2012.0046

Franz, T. E., Zreda, M., Rosolem, R., Hornbuckle, B. K., Irvin, S. L., Adams, H., et al. (2013). Ecosystem-scale measurements of biomass water using cosmic ray neutrons. *Geophysical Research Letters*, *40*(15), 3929–3933. https://doi.org/10.1002/grl.50791

García-Ruiz, J. M., López-Moreno, J. I., Vicente-Serrano, S. M., Lasanta–Martínez, T., & Beguería, S. (2011). Mediterranean water resources in a global change scenario. *Earth-Science Reviews*, *105*(3–4), 121–139. https://doi.org/10.1016/j.earscirev.2011.01.006

Gianessi, S., Polo, M., Stevanato, L., Lunardon, M., Francke, T., Oswald, S., et al. (2022). Testing a novel sensor design to jointly measure cosmic-ray neutrons, muons and gamma rays for non-invasive soil moisture estimation. *Geoscientific Instrumentation, Methods and Data Systems Discussions*, *2022*, 1–18. https://doi.org/10.5194/gi-13-9-2024

Gugerli, R., Salzmann, N., Huss, M., & Desilets, D. (2019). Continuous and autonomous snow water equivalent measurements by a cosmic ray sensor on an alpine glacier. *The Cryosphere*, *13*(12), 3413–3434. https://doi.org/10.5194/tc-13-3413-2019

Han, X., Hendricks-Franssen, H.-J., Bello, M. Á. J., Rosolem, R., Bogena, H. R., Alzamora, F. M., et al. (2016). Simultaneous soil moisture and properties estimation for a drip irrigated field by assimilating cosmic-ray neutron intensity. *Journal of Hydrology*, *539*, 611–624. https://doi.org/10.1016/j.jhydrol.2016.05.050

Hardie, M. (2020). Review of novel and emerging proximal soil moisture sensors for use in agriculture. *Sensors*, *20*(23), 6934. https://doi.org/10.3390/s20236934

Heidbüchel, I., Güntner, A., & Blume, T. (2016). Use of cosmic-ray neutron sensors for soil moisture monitoring in forests. *Hydrology and Earth System Sciences*, *20*(3), 1269–1288. https://doi.org/10.5194/hess-20-1269-2016

Heistermann, M., Francke, T., Schrön, M., & Oswald, S. E. (2021). Spatio-temporal soil moisture retrieval at the catchment scale using a dense network of cosmic-ray neutron sensors. *Hydrology and Earth System Sciences*, *25*(9), 4807–4824. https://doi.org/10.5194/hess-25-4807-2021

IPCC. (2023). *Climate change 2022 – Impacts, Adaptation and Vulnerability: Working Group II contribution to the sixth assessment report of the intergovernmental Panel on climate change*. Cambridge University Press.

Jakobi, J., Huisman, J., Vereecken, H., Diekkrüger, B., & Bogena, H. (2018). Cosmic ray neutron sensing for simultaneous soil water content and biomass quantification in drought conditions. *Water Resources Research*, *54*(10), 7383–7402. https://doi.org/10.1029/2018WR022692

Jakobi, J., Huisman, J. A., Fuchs, H., Vereecken, H., & Bogena, H. R. (2022). Potential of thermal neutrons to correct cosmic-ray neutron soil moisture content measurements for dynamic biomass effects. https://doi.org/10.1029/2022WR031972

Jakobi, J., Huisman, J. H., Schrön, M., Fiedler, J., Brogi, C., Vereecken, H., & Bogena, H. R. (2020). Error estimation for soil moisture measurements with cosmic-ray neutron sensing and implications for rover surveys. *Frontiers in Water*, *2*, 10. https://doi.org/10.3389/frwa.2020.00010

Kamali, B., Lorite, I. J., Webber, H. A., Rezaei, E. E., Gabaldon-Leal, C., Nendel, C., et al. (2022). Uncertainty in climate change impact studies for irrigated maize cropping systems in southern Spain. *Scientific Reports*, *12*(1), 1–13. https://doi.org/10.1038/s41598-022-08056-9

Kaufmann, M. S., von Hebel, C., Weihermüller, L., Baumecker, M., Döring, T., Schweitzer, K., et al. (2020). Effect of fertilizers and irrigation on multi-configuration electromagnetic induction measurements. *Soil Use & Management*, *36*(1), 104–116. https://doi.org/10.1111/sum.12530

Köhli, M. (2026). Soil moisture measurements by Cosmic-Ray neutron sensing: A critical review. *Geoderma*, *465*, 117626. https://doi.org/10.1016/j.geoderma.2025.117626

Köhli, M., Schrön, M., & Schmidt, U. (2018). Response functions for detectors in cosmic ray neutron sensing. *Nuclear Instruments and Methods in Physics Research Section A: Accelerators, Spectrometers, Detectors and Associated Equipment*, *902*, 184–189. https://doi.org/10.1016/j.nima.2018.06.052

Köhli, M., Schrön, M., Zacharias, S., & Schmidt, U. (2023). URANOS v1.0 - The ultra rapid adaptable neutron-only simulation for environmental research. *Geoscientific Model Development Discussions*, 1–48. https://doi.org/10.5194/gmd-2022-93

Köhli, M., Schrön, M., Zreda, M., Schmidt, U., Dietrich, P., & Zacharias, S. (2015). Footprint characteristics revised for field-scale soil moisture monitoring with cosmic-ray neutrons. *Water Resources Research*, *51*(7), 5772–5790. https://doi.org/10.1002/2015WR017169

Köhli, M., Weimar, J., Schrön, M., Baatz, R., & Schmidt, U. (2021). Soil moisture and air humidity dependence of the above-ground cosmic-ray neutron intensity. *Frontiers in Water*, *2*, 66. https://doi.org/10.3389/frwa.2020.544847

Kootanoor Sheshadrivasan, V., Langhammer, J., Scheiffele, L., Terschlüsen, J., & Francke, T. (2025). picoSMMS: Development and validation of a low-cost and open-source soil moisture monitoring station. *Sensors*, *25*(22), 6907. https://doi.org/10.3390/s25226907

LBGR. (2025). Landesamt Für Bergbau, Geologie Und Rohstoffe Brandenburg. *Bodenbersichtskarte Des Landes Brandenburg Im Maßstab*, *1: 300*, 000.

Li, D., Schrön, M., Kohli, M., Bogena, H. R., Weimar, J., Jiménez Bello, M. A., et al. (2019). Can drip irrigation be scheduled with cosmic-ray neutron sensing? *Vadose Zone Journal*, *18*(1), 1–13. https://doi.org/10.2136/vzj2019.05.0053

Majone, B., Viani, F., Filippi, E., Bellin, A., Massa, A., Toller, G., et al. (2013). Wireless sensor network deployment for monitoring soil moisture dynamics at the field scale. *Procedia Environmental Sciences*, *19*, 426–435. https://doi.org/10.1016/j.proenv.2013.06.049

McJannet, D., & Desilets, D. (2023). Incoming neutron flux corrections for cosmic-ray soil and snow sensors using the global neutron monitor network. *Water Resources Research*, *59*(4), e2022WR033889. https://doi.org/10.1029/2022wr033889

McJannet, D., Hawdon, A., Baker, B., Renzullo, L., & Searle, R. (2017). Multiscale soil moisture estimates using static and roving cosmic-ray soil moisture sensors. *Hydrology and Earth System Sciences*, *21*(12), 6049–6067. https://doi.org/10.5194/hess-21-6049-2017

McNeill, J. D. (1980). Electromagnetic terrain conductivity measurement at low induction numbers. In *Geonics limited Ontario*.

Milano, M., Ruelland, D., Fernandez, S., Dezetter, A., Fabre, J., Servat, E., et al. (2013). Current state of Mediterranean water resources and future trends under climatic and anthropogenic changes. *Hydrological Sciences Journal*, *58*(3), 498–518. https://doi.org/10.1080/02626667.2013.774458

Mohanty, B. P., Cosh, M. H., Lakshmi, V., & Montzka, C. (2017). Soil moisture remote sensing: State-of-the-science. *Vadose Zone Journal*, *16*(1), 1–9. https://doi.org/10.2136/vzj2016.10.0105

Molden, D. (2013). *Water for food water for life: A comprehensive assessment of water management in agriculture*. Routledge. https://doi.org/10.4324/9781849773799

Montzka, C., Bogena, H. R., Zreda, M., Monerris, A., Morrison, R., Muddu, S., & Vereecken, H. (2017). Validation of spaceborne and modelled surface soil moisture products with cosmic-ray neutron probes. *Remote Sensing*, *9*(2), 103. https://doi.org/10.3390/rs9020103

Ney, P., Köhli, M., Bogena, H. R., & Goergen, K. (2021). CRNS-based monitoring technologies for a weather and climate-resilient agriculture: Realization by the ADAPTER project. *IEEE International Workshop on Metrology for Agriculture and Forestry (MetroAgriFor)*. https://doi.org/10.1109/MetroAgriFor52389.2021.9628766

Nieberding, F., Huisman, J. A., Huebner, C., Schilling, B., Weuthen, A., & Bogena, H. R. (2023). Evaluation of three soil moisture profile sensors using laboratory and field experiments. *Sensors*, *23*(14), 6581. https://doi.org/10.3390/s23146581

Nrw, G. D. (2025). Bodenkarte zur Standorterkundung 1 : 5 000. Retrieved 24.11.2025 from https://www.gd.nrw.de/pr_kd_bodenkarte-5000.php

Peng, J., Albergel, C., Balenzano, A., Brocca, L., Cartus, O., Cosh, M. H., et al. (2021). A roadmap for high-resolution satellite soil moisture applications–confronting product characteristics with user requirements. *Remote Sensing of Environment*, *252*, 112162. https://doi.org/10.1016/j.rse.2020.112162

Pisinaras, V., Herrmann, F., Panagopoulos, A., Tziritis, E., McNamara, I., & Wendland, F. (2023). Fully distributed water balance modelling in large agricultural areas—The pinios river basin (Greece) case study. *Sustainability*, *15*(5), 4343. https://doi.org/10.3390/su15054343

Pisinaras, V., Paraskevas, C., & Panagopoulos, A. (2021). Investigating the effects of agricultural water management in a Mediterranean coastal aquifer under Current and projected climate conditions. *Water*, *13*(1), 108. https://doi.org/10.3390/w13010108

Power, D., Zacharias, S., Erxleben, F., Rosolem, R., & Schrön, M. (2025). Neptoon: An extensible software tool for CRNS data processing. eLTER Science Conference 2025 Proceedings. https://doi.org/10.3897/aca.8.e158417

Pramanik, M., Khanna, M., Singh, M., Singh, D., Sudhishri, S., Bhatia, A., & Ranjan, R. (2022). Automation of soil moisture sensor-based basin irrigation system. *Smart Agricultural Technology*, *2*, 100032. https://doi.org/10.1016/j.atech.2021.100032

Puma, M., & Cook, B. (2010). Effects of irrigation on global climate during the 20th century. *Journal of Geophysical Research*, *115*(D16). https://doi.org/10.1029/2010JD014122

Ragab, R., Evans, J. G., Battilani, A., & Solimando, D. (2017). The cosmic-ray soil moisture observation system (Cosmos) for estimating the crop water requirement: New approach. *Irrigation and Drainage*, *66*(4), 456–468. https://doi.org/10.1002/ird.2152

Rasche, D., Blume, T., & Güntner, A. (2024). Depth extrapolation of field-scale soil moisture time series derived with cosmic-ray neutron sensing (CRNS) using the soil moisture analytical relationship (SMAR) model. *Soils*, *10*(2), 655–677. https://doi.org/10.5194/soil-10-655-2024

Rasche, D., Köhli, M., Schrön, M., Blume, T., & Güntner, A. (2021). Towards disentangling heterogeneous soil moisture patterns in cosmic-ray neutron sensor footprints. *Hydrology and Earth System Sciences*, *25*(12), 6547–6566. https://doi.org/10.5194/hess-25-6547-2021

Rosolem, R., Hoar, T., Arellano, A., Anderson, J. L., Shuttleworth, W. J., Zeng, X., & Franz, T. E. (2014). Translating aboveground cosmic-ray neutron intensity to high-frequency soil moisture profiles at sub-kilometer scale. *Hydrology and Earth System Sciences*, *18*(11), 4363–4379. https://doi.org/10.5194/hess-18-4363-2014

Rosolem, R., Shuttleworth, W. J., Zreda, M., Franz, T. E., Zeng, X., & Kurc, S. A. (2013). The effect of atmospheric water vapor on neutron count in the cosmic-ray soil moisture observing system. *Journal of Hydrometeorology*, *14*(5), 1659–1671. https://doi.org/10.1175/JHM-D-12-0120.1

Rost, S., Gerten, D., Bondeau, A., Lucht, W., Rohwer, J., & Schaphoff, S. (2008). Agricultural green and blue water consumption and its influence on the global water system. *Water Resources Research*, *44*(9). https://doi.org/10.1029/2007WR006331

Schattan, P., Baroni, G., Oswald, S. E., Schöber, J., Fey, C., Kormann, C., et al. (2017). Continuous monitoring of snowpack dynamics in alpine terrain by aboveground neutron sensing. *Water Resources Research*, *53*(5), 3615–3634. https://doi.org/10.1002/2016WR020234

Schattan, P., Köhli, M., Schrön, M., Baroni, G., & Oswald, S. E. (2019). Sensing area-average snow water equivalent with cosmic-ray neutrons: The influence of fractional snow cover. *Water Resources Research*, *55*(12), 10796–10812. https://doi.org/10.1029/2019WR025647

Schattan, P., Schwaizer, G., Schöber, J., & Achleitner, S. (2020). The complementary value of cosmic-ray neutron sensing and snow covered area products for snow hydrological modelling. *Remote Sensing of Environment*, *239*, 111603. https://doi.org/10.1016/j.rse.2019.111603

Scheiffele, L. M., Baroni, G., Franz, T. E., Jakobi, J., & Oswald, S. E. (2020). A profile shape correction to reduce the vertical sensitivity of cosmic-ray neutron sensing of soil moisture. *Vadose Zone Journal*, *19*(1), e20083. https://doi.org/10.1002/vzj2.20083

Schmäck, J., Weihermüller, L., Klotzsche, A., von Hebel, C., Pätzold, S., Welp, G., & Vereecken, H. (2022). Large-scale detection and quantification of harmful soil compaction in a post-mining landscape using multi-configuration electromagnetic induction. *Soil Use & Management*, *38*(1), 212–228. https://doi.org/10.1111/sum.12763

Schrön, M., Köhli, M., Scheiffele, L., Iwema, J., Bogena, H. R., Lv, L., et al. (2017). Improving calibration and validation of cosmic-ray neutron sensors in the light of spatial sensitivity. *Hydrology and Earth System Sciences*, *21*(10), 5009–5030. https://doi.org/10.5194/hess-21-5009-2017

Schrön, M., Köhli, M., & Zacharias, S. (2023). Signal contribution of distant areas to cosmic-ray neutron sensors - Implications on footprint and sensitivity. *EGUsphere*, *2022*, 1–25. https://doi.org/10.5194/egusphere-2022-219

Schrön, M., Oswald, S. E., Zacharias, S., Kasner, M., Dietrich, P., & Attinger, S. (2021). Neutrons on rails: Transregional monitoring of soil moisture and snow water equivalent. *Geophysical Research Letters*, *48*(24), e2021GL093924. https://doi.org/10.1029/2021GL093924

Scudiero, E., Corwin, D. L., Markley, P. T., Pourreza, A., Rounsaville, T., Bughici, T., & Skaggs, T. H. (2024). A system for concurrent on-the-go soil apparent electrical conductivity and gamma-ray sensing in micro-irrigated orchards. *Soil and Tillage Research*, *235*, 105899. https://doi.org/10.1016/j.still.2023.105899

Serafini, A., Albéri, M., Amoretti, M., Anconelli, S., Bucchi, E., Caselli, S., et al. (2021). Proximal gamma-ray spectroscopy: An effective tool to discern rain from irrigation. *Remote Sensing*, *13*(20), 4103. https://doi.org/10.3390/rs13204103

Shuttleworth, J., Rosolem, R., Zreda, M., & Franz, T. (2013). The COsmic-ray Soil Moisture Interaction Code (COSMIC) for use in data assimilation. *Hydrology and Earth System Sciences*, *17*(8), 3205–3217. https://doi.org/10.5194/hess-17-3205-2013

Strati, V., Albéri, M., Anconelli, S., Baldoncini, M., Bittelli, M., Bottardi, C., et al. (2018). Modelling soil water content in a tomato field: Proximal gamma ray spectroscopy and soil–crop system models. *Agriculture*, *8*(4), 60. https://doi.org/10.3390/agriculture8040060

Tian, Z., Li, Z., Liu, G., Li, B., & Ren, T. (2016). Soil water content determination with cosmic-ray neutron sensor: Correcting aboveground hydrogen effects with thermal/fast neutron ratio. *Journal of Hydrology*, *540*, 923–933. https://doi.org/10.1016/j.jhydrol.2016.07.004

Topp, G. C., Davis, J. L., & Annan, A. P. (1980). Electromagnetic determination of soil water content: Measurements in coaxial transmission lines. *Water Resources Research*, *16*(3), 574–582. https://doi.org/10.1029/wr016i003p00574

Troy, T. J., Kipgen, C., & Pal, I. (2015). The impact of climate extremes and irrigation on US crop yields. *Environmental Research Letters*, *10*(5), 054013. https://doi.org/10.1088/1748-9326/10/5/054013

Uhlenbrook, S. (2019). The United Nations world water development report 2019: Leaving no one behind.

URANOS. (2025). Uranos. Retrieved from https://gitlab.com/mkoehli/uranos/-/blob/main/doc/PUBLICATIONS.md

Van Vliet, M. T., Jones, E. R., Flörke, M., Franssen, W. H., Hanasaki, N., Wada, Y., & Yearsley, J. R. (2021). Global water scarcity including surface water quality and expansions of clean water technologies. *Environmental Research Letters*, *16*(2), 024020. https://doi.org/10.1088/1748-9326/abbfc3

Vereecken, H., Huisman, J. A., Bogena, H., Vanderborght, J., Vrugt, J. A., & Hopmans, J. W. (2008). On the value of soil moisture measurements in vadose zone hydrology: A review. *Water Resources Research*, *44*(4). https://doi.org/10.1029/2008WR006829

von Hebel, C., Matveeva, M., Verweij, E., Rademske, P., Kaufmann, M. S., Brogi, C., et al. (2018). Understanding soil and plant interaction by combining ground-based quantitative electromagnetic induction and airborne hyperspectral data. *Geophysical Research Letters*, *45*(15), 7571–7579. https://doi.org/10.1029/2018GL078658

von Hebel, C., Rudolph, S., Mester, A., Huisman, J. A., Kumbhar, P., Vereecken, H., & van der Kruk, J. (2014). Three-dimensional imaging of subsurface structural patterns using quantitative large-scale multiconfiguration electromagnetic induction data. *Water Resources Research*, *50*(3), 2732–2748. https://doi.org/10.1002/2013WR014864

Wagner, W., Blöschl, G., Pampaloni, P., Calvet, J.-C., Bizzarri, B., Wigneron, J.-P., & Kerr, Y. (2007). Operational readiness of microwave remote sensing of soil moisture for hydrologic applications. *Hydrology Research*, *38*(1), 1–20. https://doi.org/10.2166/nh.2007.029

Walker, J. P., Houser, P. R., & Willgoose, G. R. (2004). Active microwave remote sensing for soil moisture measurement: A field evaluation using ERS-2. *Hydrological Processes*, *18*(11), 1975–1997. https://doi.org/10.1002/hyp.1343

Weimar, J., Köhli, M., Budach, C., & Schmidt, U. (2020). Large-Scale Boron-Lined Neutron Detection Systems as a 3He Alternative for Cosmic Ray Neutron Sensing [Original Research]. *Frontiers in Water*, *2*, 16. https://doi.org/10.3389/frwa.2020.00016

Western, A. W., Grayson, R. B., & Blöschl, G. (2002). Scaling of soil moisture: A hydrologic perspective. *Annual Review of Earth and Planetary Sciences*, *30*(1), 149–180. https://doi.org/10.1146/annurev.earth.30.091201.140434

Wichelns, D., & Qadir, M. (2015). Achieving sustainable irrigation requires effective management of salts, soil salinity, and shallow groundwater. *Agricultural Water Management*, *157*, 31–38. https://doi.org/10.1016/j.agwat.2014.08.016

Zhu, Z., Tan, L., Gao, S., & Jiao, Q. (2014). Observation on soil moisture of irrigation cropland by cosmic-ray probe. *IEEE Geoscience and Remote Sensing Letters*, *12*(3), 472–476. https://doi.org/10.1109/LGRS.2014.2346784

Zreda, M., Desilets, D., Ferré, T. P. A., & Scott, R. L. (2008). Measuring soil moisture content non-invasively at intermediate spatial scale using cosmic-ray neutrons. *Geophysical Research Letters*, *35*(21). https://doi.org/10.1029/2008GL035655

Zreda, M., Shuttleworth, W. J., Zeng, X., Zweck, C., Desilets, D., Franz, T., & Rosolem, R. (2012). COSMOS: The cosmic-ray soil moisture observing system. *Hydrology and Earth System Sciences*, *16*(11), 4079–4099. https://doi.org/10.5194/hess-16-4079-2012